Figure 2 Ang1 induces *trans*-association of Tie2 at cell–cell contacts. (a) *In vitro* binding of sTie2–HA to sTie1–Fc or sTie2–Fc. Binding in the presence or absence of COMP-Ang1 was examined as described in Methods. Arrows indicate co-precipitated sTie2–HA and COMP-Ang1 proteins. (b) The association of sTie2–HA to sTie2–Fc by Ang1, GCN4–Ang1, MAT–Ang1, or COMP-Ang1 was similarly examined as in a. (c) Confluent HUVECs were stimulated with vehicle (control), 200 ng ml⁻¹ GCN4–Ang1, MAT–Ang1 or COMP-Ang1 for 20 min, and stained with anti-Tie2 (upper panels) and anti-VE-cadherin (lower panels) antibodies. The scale bars represent 20 μm. (d) Aggregation of 293F cells in suspension expressing GFP, Tie2–GFP, Tie2Δcyto–GFP and Tie2KD–GFP was induced by vehicle (control; left of each panel) and COMP-Ang1 (right of each panel), as described in Methods. Upper and lower images of each panel show the phase-contrast and GFP images. (e) To quantify the cell aggregation observed in d, the number of cell aggregates per field of view was counted. An aggregate was defined as cell mass consisting of more than 4 cells. The number of aggregates for cells stimulated with vehicle and COMP-Ang1 is shown as white and black columns, respectively. Data are expressed as mean number ± s.d. of, at least, 10 different fields. (f) 293F cells expressing Tie2Δcyto–GFP were incubated with vehicle (control; left column) and COMP-Ang1 (right column). Upper and lower panels show the confocal GFP images merged without or with the DIC images, respectively. The scale bars represent 10 μm. (g) 293F cells expressing Tie2Δcyto–HA were suspended with either those expressing Tie2Δcyto–GFP or those expressing GFP, and stimulated with 400 ng ml⁻¹ of COMP-Ang1 for 1 h. Cell lysates were immunoprecipitated with anti-GFP antibody. Immunoprecipitates (IP) and aliquots of cell lysate (TCL) were subjected to Western blot analysis (WB) with anti-HA and anti-GFP antibodies. Uncropped images of a, b, and g are shown in Supplementary Information, Fig. S8.

fused with green fluorescent protein (GFP) (Tie2–GFP) (Supplementary Information, Fig. S1g, h and Movie 1).

VEGFR2 is known to associate with VE-cadherin at cell–cell contacts[21,22]. Thus, we assumed that VE-cadherin might be involved in

Tie2 relocation to cell–cell contacts. However, Tie2 relocation at cell–cell contacts was still observed in VE-cadherin–depleted HUVECs, while β-catenin disappeared from cell–cell contacts (Supplementary Information, Fig. S2a, c). Tie2 staining at cell–cell contacts was slightly
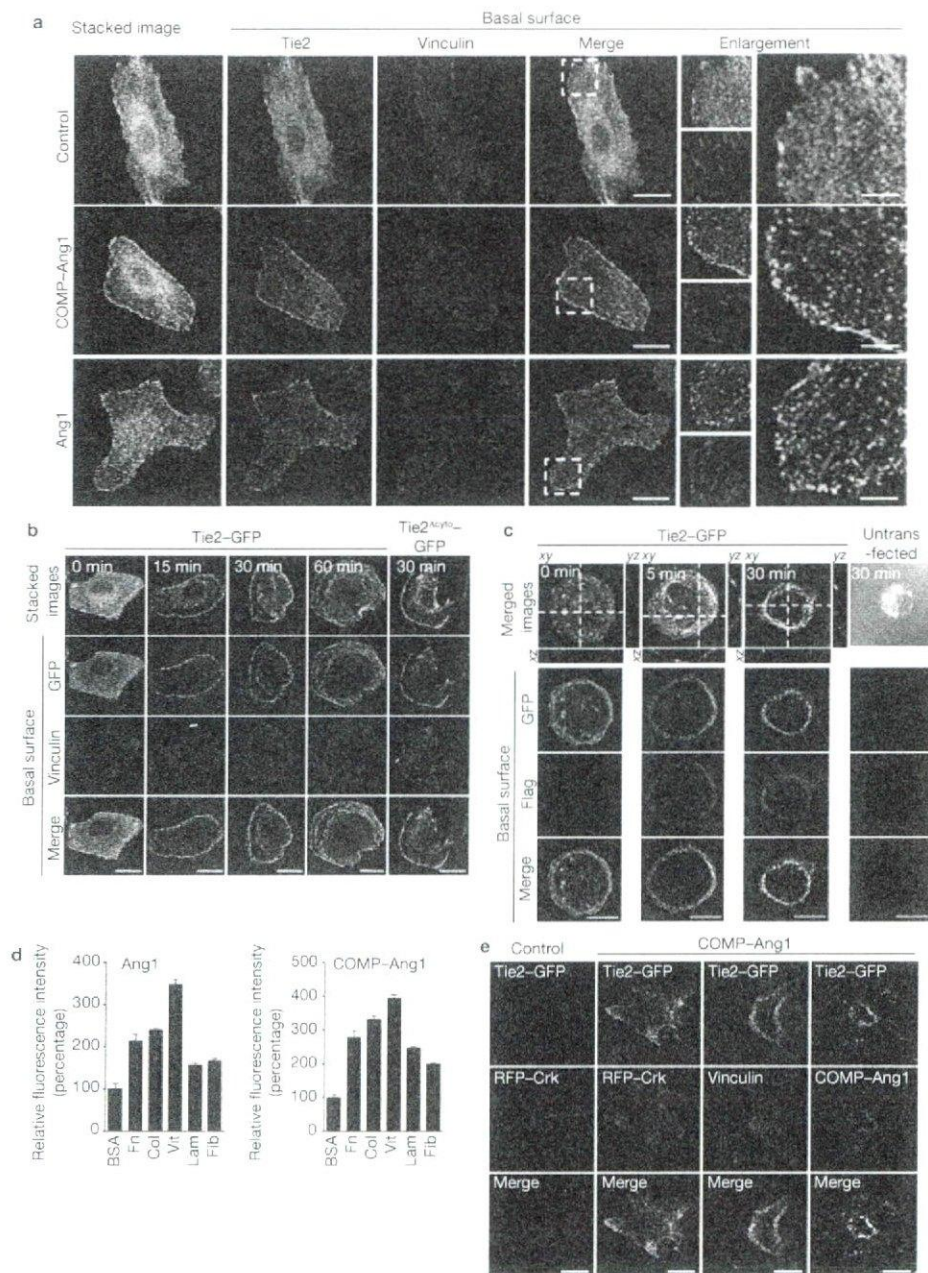
Figure 3 ECM-bound Ang1 anchors Tie2 to cell–substratum contacts in the absence of cell–cell adhesions. (**a**) Sparse HUVECs were stimulated with vehicle (control), COMP–Ang1 or Ang1, and then immunostained with anti-Tie2 and anti-vinculin antibodies. Images were obtained using a confocal microscope. Stacked xy images (left), Tie2 (green), vinculin (red) and merged (merge) images of the cell–substratum interface (basal surface) are shown. The boxed areas in the merged images are enlarged (right panels). (**b**) Time course (for the time indicated) of localization of Tie2–GFP and vinculin in CHO cells expressing Tie2–GFP was examined similarly to a. Localization of Tie2Δcyto–GFP after stimulation for 30 min was also examined (left column). (**c**) Localization of COMP–Ang1 (Flag, red) and Tie2–GFP (green) after stimulation with COMP–Ang1 in CHO cells expressing Tie2–GFP was examined similarly to **a**. Untransfected CHO cells were also stimulated with COMP–Ang1, and immunostained with anti-Flag antibody (right column). A DIC image (top) is displayed at the top. (**d**) Binding of Ang1 and COMP–Ang1 to ECM was examined by immunofluorescence analysis as described in

Supplementary Methods. Glass-base dishes were coated with BSA (BSA), fibronectin (Fn), collagen (Col), vitronectin (Vit), laminin (Lam), and fibrinogen (Fib), and incubated with Ang1 (left panel) or COMP–Ang1 (right panel). ECM-bound Ang1 and COMP–Ang1 were detected by staining with anti-Flag antibody. Relative immunofluorescence intensity was expressed as a percentage of that detected in a BSA-coated dish. Data are expressed as mean ± s.d. of the fluorescence intensity of 6 different fields. (**e**) Sparse HUVECs expressing both Tie2–GFP and RFP–Crk and those expressing Tie2–GFP were stimulated with COMP–Ang1 or vehicle (control). After stimulation for 20 min, the cells were washed and treated with cytoskeleton stabilizing buffer as described in Methods. The cells expressing Tie2–GFP were immunostained with either anti-vinculin or anti-Flag antibody. GFP (Tie2–GFP), and RFP (RFP–Crk) or Alexa 546 (vinculin or COMP–Ang1) confocal images of the cell–substratum interface, and merged images (bottom) are shown. The scale bars in merged (**a**, **b**, **c**, and **e**) and enlarged images (**a**) represent 20 μm and 5 μm, respectively.

diminished compared to the control cells. Consistently, we found that Tie2 did not co-immunoprecipitate with VE-cadherin in the COMP–Ang1-stimulated HUVECs, although VEGFR2 co-immunoprecipitated with VE-cadherin in those stimulated by VEGF (Supplementary Information, Fig. S2d, e). Furthermore, depletion of platelet and endothelial cell adhesion molecule-1 (PECAM-1) did not affect the relocation of Tie2 to cell–cell contacts (Supplementary Information, Fig. S2b, c). These results indicate that VE-cadherin and PECAM-1 are not essential for Tie2 localization at cell–cell contacts, although cell adhesions by these molecules may affect the localization of Tie2 by stabilizing cell–cell contacts.

We hypothesized that the interaction of Tie2 expressed in adjoining cells might be required for the accumulation of Tie2 at cell–cell contacts. We employed Chinese hamster ovary (CHO) cells that do not express endogenous Tie2 and CHO cells expressing Tie2–GFP. By monitoring Tie2–GFP upon COMP–Ang1 stimulation, we could distinguish the dynamics of Tie2–GFP in the presence or absence of Tie2 expression between adjoining CHO cells. Tie2–GFP was internalized upon stimulation with COMP–Ang1 when a Tie2–GFP-expressing cell was surrounded by wild-type CHO cells (Fig. 1b and Supplementary Information, Movie2). In contrast, COMP–Ang1 stimulation induced Tie2–GFP translocation to the cell–cell borders between adjacent cells expressing Tie2–GFP, although Tie2–GFP was homogeneously expressed on the plasma membrane before the stimulation (Fig. 1c and Supplementary Information, Fig. S2f and Movie3). Notably, Tie2–GFP lacking the cytoplasmic domain of Tie2 (Tie2Δcyto–GFP) relocated to the borders between adjacent cells expressing Tie2Δcyto–GFP (Fig. 1d and Supplementary Information, Movie 4). To further test the effect of the extracellular domain of Tie2 between adjoining cells on the accumulation of Tie2 at cell–cell contacts, CHO cells expressing Tie2Δcyto–GFP and those expressing Tie2Δcyto–HA (a mutant Tie2 lacking the cytoplasmic domain tagged with HA) were co-plated and stimulated with COMP–Ang1. In the unstimulated cells, both Tie2Δcyto–GFP and Tie2Δcyto–HA were broadly expressed on the plasma membrane without any colocalization. Once stimulated with COMP–Ang1, Tie2Δcyto–GFP and Tie2Δcyto–HA colocalized at the cell–cell borders between cells expressing Tie2Δcyto–GFP and cells expressing Tie2Δcyto–HA (Fig. 1e). Interestingly, COMP–Ang1 was also detected at the cell–cell borders where Tie2Δcyto–GFP localized (Fig. 1f). Collectively, these findings suggest that Ang1 induces trans-association of Tie2 at cell–cell contacts independently of its intracellular signalling.

Internalization was further analysed by a confocal microscope. In Tie2–GFP-expressing CHO cells surrounded by wild-type CHO cells, Tie2–GFP was clearly internalized upon COMP–Ang1 stimulation, while in either Tie2Δcyto–GFP-expressing CHO cells or kinase-negative Tie2–GFP (Tie2KD–GFP)-expressing CHO cells, Tie2 was not internalized (Supplementary Information, Fig. S2g). These data indicate that endocytosis of Tie2 is triggered by its intracellular signalling, and suggest that Ang1-induced localization of Tie2 at cell–cell contacts depends upon the balance between trans-association of activated Tie2 and the internalization of Tie2.

Trans-association of Tie2 induced by oligomerized Ang1

To explore whether the trans-association of Tie2 is provoked by oligomerized Ang1, we first biochemically analysed the association of Tie2 using recombinant Tie proteins. We tested the association of immunoglobulin
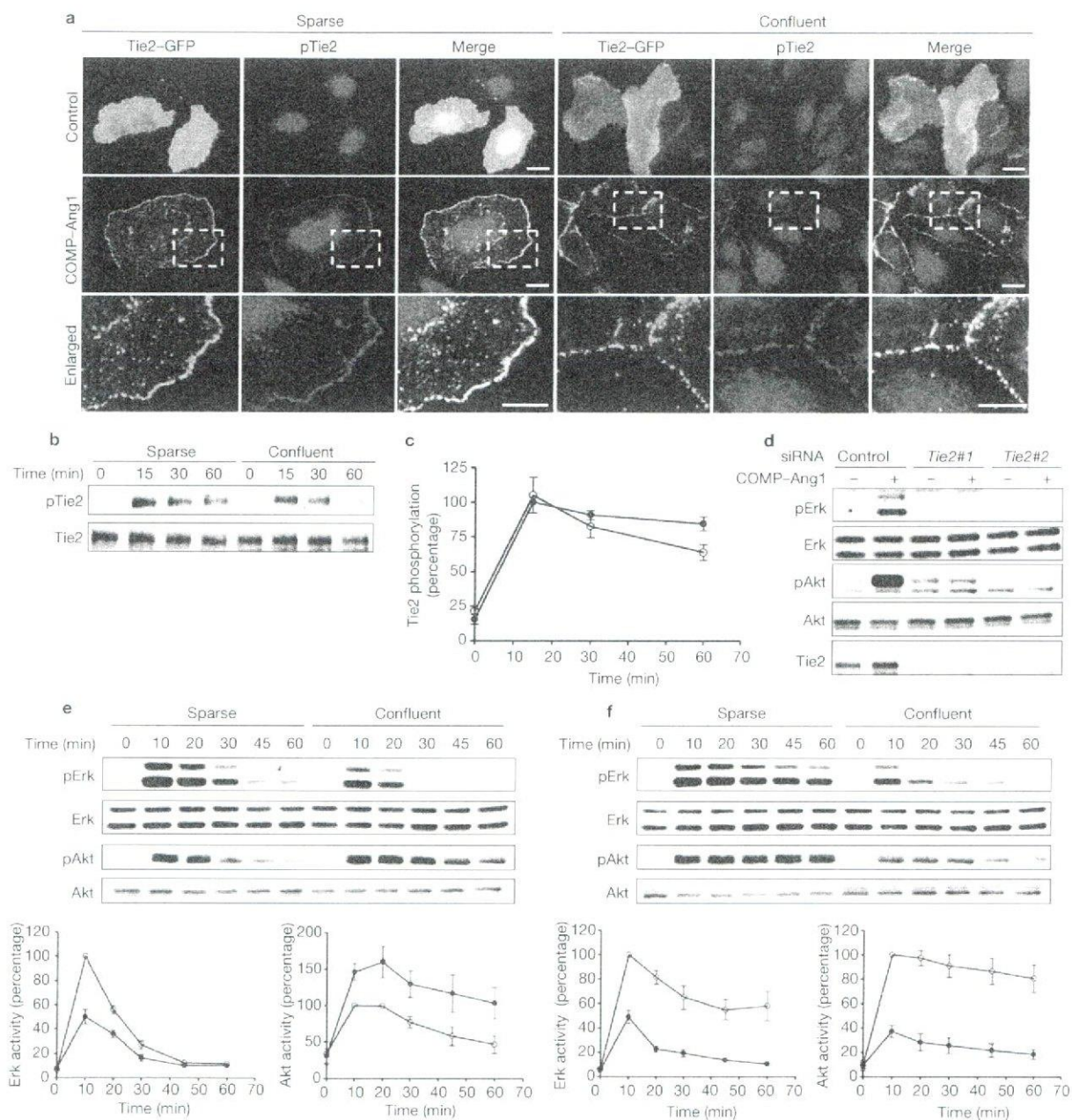
Fc-domain tagged extracellular domain of either Tie1 or Tie2 with the HA-tagged extracellular domain of Tie2, as explained in Supplementary Fig. 3a and 3b. HA-tagged Tie2 bound to sTie2–Fc but not sTie1–Fc in the presence of COMP–Ang1 (Fig. 2a). We then tested the association of sTie2–HA with sTie2–Fc in the presence of various forms of Ang1 (GCN4–Ang1, dimer; native Ang1 and MAT-Ang1, tetramer; COMP–Ang1, pentamer)[14]. The association of sTie2–HA with sTie2–Fc was induced by native Ang1, MAT-Ang1, and COMP–Ang1, which can form multimers of Ang1, but not by GCN4–Ang1 (Fig. 2b). Consistently, multimerized Ang1 induced the relocation of Tie2 at cell–cell contacts (Fig. 2c).

We further tested the possibility of Ang1-mediated bridging of Tie2 by using 293 cells in suspension (293F). Tie2–GFP-expressing 293F cells but not GFP-expressing 293F cells aggregated upon COMP–Ang1 and native Ang1 stimulation (Fig. 2d, e and Supplementary Information, Fig. S3c, d). The number of aggregates in Tie2–GFP-expressing cells increased more than in Tie2Δcyto–GFP-expressing cells and Tie2KD–GFP-expressing cells that were resistant to internalization of Tie2 (Fig. 2e and Supplementary Information, Fig. S2g). In contrast, the size of the aggregates was increased in Tie2Δcyto–GFP-expressing cells and Tie2KD–GFP-expressing cells compared to Tie2–GFP-expressing cells (Supplementary Information, Fig. S3e), suggesting that intracellular signalling may affect Ang1-mediated Tie2 trans-association probably through Tie2 internalization.

In the aggregated cells, Tie2Δcyto–GFP clearly localized at the sites of cell–cell contacts (Fig. 2f). Similar localization of Tie2Δcyto–GFP at cell–cell contacts was observed in a murine pro-B cell line, BaF3 cells, stably expressing Tie2Δcyto–GFP (BaF–Tie2ΔcytoGFP) upon COMP–Ang1 stimulation (Supplementary Information, Fig. S3h). VEGF did not induce aggregation of 293F cells expressing VEGFR2, although VEGFR2 is reported to localize to cell–cell contacts[21,23] (Supplementary Information, Fig. S3f, g). When 293F cells expressing Tie2Δcyto–GFP and those expressing Tie2Δcyto–HA were co-cultured in suspension and stimulated with COMP–Ang1, both Tie2 were co-immunoprecipitated (Fig. 2g). Furthermore, when BaF–Tie2ΔcytoGFP cells and BaF3 cells stably expressing Tie2Δcyto–HA (BaF–Tie2ΔcytoHA) were mixed and stimulated with COMP–Ang1 in suspension, both truncated forms of Tie2 were also co-immunoprecipitated (Supplementary Information, Fig. S3i). These results together with biochemical data and the co-localization of Tie2 lacking its cytoplasmic domain (Fig. 1e) indicate the trans-association of Tie2 occurs at cell–cell contacts upon oligomerized Ang1 stimulation.

Tie2 localizes to cell–substratum contacts in the absence of cell–cell contacts

We next examined Ang1-induced localization of Tie2 in sparse HUVECs. In subconfluent HUVECs, Tie2 was preferentially recruited to cell–cell contacts upon COMP–Ang1 stimulation (Supplementary Information, Fig. S4a). However, when stimulated in the absence of cell–cell contacts, Tie2 localized to the periphery of the extended membrane that was close to but different from vinculin- and paxillin-positive focal complexes (FCs) (Fig. 3a and Supplementary Information, Fig. S4b). We further investigated COMP–Ang1-induced localization of Tie2–GFP in CHO cells. Tie2–GFP was localized to the periphery at 15, 30 and 60 min after stimulation. We noticed additional GFP-positive lines at cell–substratum contacts in the cells stimulated for 30 min and 60 min, reflecting the footprints of membrane extension during cell movement (Fig. 3b).

Figure 4 *Trans*-association of Tie2 leads to the preferential activation of Akt. (a) Sparse and confluent HUVECs were transfected with the plasmid encoding Tie2–GFP, stimulated with either vehicle (control) or COMP–Ang1, and immunostained with an anti-phospho Tie2 (pTie2) antibody. Images of Tie2–GFP (green), pTie2 (red), and the merged images (merge) are shown. The boxed areas in the panels are enlarged at the bottom of each image. The scale bars in the merged and the enlarged images represent 20 and 5 μm, respectively. (b) Sparse and confluent HUVECs were starved and stimulated with COMP–Ang1 for the time (min) indicated at the top. Cell lysates were immunoprecipitated with anti-Tie2 antibody. Immunoprecipitates and aliquots of cell lysate were subjected to western blot analysis with anti-phosphotyrosine (pTie2) and anti-Tie2 (Tie2) antibodies. (c) Phosphorylated Tie2 observed in b was quantified. Tie2 phosphorylation represents the ratio of phosphorylated Tie2 to total Tie2 as a percentage of the ratio in the sparse cells stimulated for 15 min. Values are expressed as means ± s.d. from five independent

experiments. (d) HUVECs transfected with control siRNA (control) or with two independent siRNAs targeting different sequences of *Tie2* (Tie2 No.1 and Tie2 No.2) were starved and stimulated with vehicle (–) and COMP–Ang1 (+) for 15 min. Cell lysates were subjected to immunoblot analysis for analysing Erk and Akt phosphorylation. (e) Sparse and confluent HUVECs were stimulated with COMP–Ang1 for the time (min) indicated at the top. Activation of Erk and Akt was analysed. Graphs at the bottom left and right panels show time course of Erk and Akt activation of the sparse cells (open circle) and the confluent cells (filled circle) in response to COMP–Ang1. Erk or Akt activity represents the ratio of phospho-Erk or phospho-Akt to total Erk or total Akt as a percentage of the ratio observed in sparse cells stimulated for 10 min, respectively. Values are expressed as means ± s.d. from five independent experiments. (f) Sparse (open circle) and confluent (filled circle) HUVECs were stimulated with growth media and analysed. Uncropped images of b, d, e, f are shown in Supplementary Information, Fig. S8.

Likewise, in Tie2Δcyto–GFP-expressing CHO cells, Tie2Δcyto–GFP was found at cell–substratum contacts, indicating the requirement of the extracellular domain of Tie2 for this localization. These Tie2–GFP positive structures at cell–substratum contacts were located close to, but apparently different from, vinculin-marked FCs or focal adhesions (FAs) (Supplementary Information, Fig. S4c). To identify the cell matrix junctions where Tie2 localizes, we carefully compared Tie2–GFP with those of various markers for FCs and FAs in HUVECs plated on fibronectin- and collagen-coated dishes after COMP–Ang1 stimulation. Tie2–GFP at cell–substratum contacts colocalized with none of these markers including vinculin, paxillin, VASP, and talin (Supplementary Information, Fig. S5a–g). Collectively, these results indicate that upon stimulation with Ang1, Tie2 is recruited to the cell periphery and anchored to substratum contacts that are different from FCs and FAs. This is further supported by time-lapse imaging using HUVECs expressing Tie2–GFP and CHO cells expressing either Tie2–GFP or Tie2Δcyto–GFP upon COMP–Ang1 stimulation (Supplementary Information, Movie 6 and 7).

$\alpha_5\beta_1$ integrin associates with fibronectin fibrils to form distinct adhesive structures from FCs and FAs, namely fibrillar adhesions (FBs) where fibrinogenesis occurs[24,25]. Since Cascone et al. has reported that Tie2 constitutively associates with $\alpha_5\beta_1$ integrin that binds to fibronectin[26], we examined whether Tie2 localizes at FBs. When Tie2–GFP- or HA-tagged Tie2 (Tie2–HA)–expressing HUVECs plated on a fibronectin-coated dish were stimulated with COMP–Ang1, Tie2 did not colocalize with FB markers (α_5 integrin, assembled fibronectin fibrils and exogenously expressed GFP–tensin) (Supplementary Information, Fig. S5h–j). In addition, depletion of α_5 integrin by siRNA did not affect COMP–Ang1-induced Tie2 localization at cell–substratum contacts (Supplementary Information, Fig. S6a–d). Depletion of another integrin, $\alpha_v\beta_3$, did not alter COMP–Ang1-induced relocation of Tie2 to peripheral cell–substratum contacts (Supplementary Information, Fig. S6 a–c).

We assumed that Ang1 might anchor Tie2 to extracellular matrix (ECM). When Tie2–GFP-expressing CHO cells were sparsely cultured on collagen-coated dishes and stimulated with COMP–Ang1, Tie2–GFP and FLAG-tagged COMP–Ang1 were clearly colocalized at the periphery and bottom of the cells at 5 min after stimulation, with the appearace of a ring (Fig. 3c). After 30 min, we noticed that Ang1 was detected not only with Tie2–GFP but also on the dish surface where the cell was not present (Fig. 3c and Supplementary Information, Fig. S6e), suggesting that Ang1 can bind to ECM. Indeed, Ang1 and COMP–Ang1, but not control protein, could bind to fibronectin, collagen, and vitronectin with high affinity, and bind weakly to laminin and fibrinogen as demonstrated by an ECM–Ang1 binding assay (Fig. 3d and Supplementary Information, Fig. S6f). Adhesive structures formed at cell–substratum contacts such as FCs and FAs are resistant to detergent (0.5% Triton-X100)[27,28]. Whereas Tie2–GFP but not RFP-Crk disappeared upon detergent addition without pretreatment of COMP–Ang1, pretreatment of COMP–Ang1 preserved Tie2–GFP at the bottom of cells as well as RFP-Crk and vinculin (Fig. 3e). These results suggest that Tie2 is anchored by ECM-bound Ang1 to cell–substratum contacts to form novel detergent-resistant adhesive structures, which are different from FCs, FAs and FBs.

Preferential activation of Erk and Akt in the absence and presence of cell–cell contacts upon Ang1 stimulation

We investigated the biological significance of trans-associated Tie2 at cell–cell contacts and cell–substratum contact-anchored Tie2 upon Ang1 stimulation. Tie2 under both conditions was phosphorylated at either cell–cell contacts or cell–substratum contacts (Fig. 4a). The extent of Tie2 phosphorylation in HUVECs by COMP–Ang1 did not depend upon the presence of cell–cell contacts (Fig. 4b, c).

Among Tie2-mediated signalling factors[1,19], Akt and Erk are suggested to be important for cell survival, and cell migration and proliferation, respectively[9,29,18,30,31]. We therefore checked the requirement of Tie2 in Ang1-induced Erk and Akt activation in HUVECs, because Ang1 is known to mediate some biological functions through integrins[32,33]. Ang1-dependent phosphorylation of both Erk and Akt in confluent and sparse HUVECs was abolished by depletion of Tie2 (Fig. 4d and data not shown). Under either sparse or confluent culture conditions, COMP–Ang1 induced Erk phosphorylation, which peaked at 10 min after stimulation and declined to the basal level by 45 min (Fig. 4e). However, the maximum level of Erk phosphorylation in the confluent cells was reduced to approximately 50% of that in the sparse cells (Fig. 4e). In clear contrast, the maximum increase in Akt phosphorylation was significantly higher in the confluent cells than in the sparse cells (Fig. 4e), indicating that endothelial cell–cell adhesions positively regulate the Tie2-mediated Akt pathway. We noticed that this preferential activation of Akt was a Tie2-specific signal in the confluent cell culture, because both Erk and Akt activation was suppressed when the endothelial cells were stimulated with growth media in the presence of cell–cell contacts (Fig. 4f).

Activation of Erk by Tie2 at cell–substratum contacts is partly dependent upon focal adhesion kinase and involved in endothelial cell migration

To further explore how Tie2-mediated signalling in isolated cells is influenced by its targeting to cell–substratum contacts, HUVECs were stimulated with COMP–Ang1 under either suspended or substratum-attached conditions. While Tie2 phosphorylation and subsequent Akt activation were comparable between these conditions, Erk activation was higher in substratum-attached cells (Fig. 5a). Similar results were obtained using BaF3 cells stably expressing Tie2 (BaF–Tie2) (Supplementary Information, Fig. S7a–c). These findings suggest that Erk activation by Ang1–Tie2 requires the contacts between cells and substratum, as previously reported for other receptor tyrosine kinases[34,35].

We hypothesized that Ang1–Tie2 at cell–substratum contacts cooperatively function with integrin signalling complexes to induce Erk activation, although Tie2 localized to cell–substratum contacts besides FCs, FAs and FBs. To test this possibility, we examined whether ECM-anchored Ang1 induces Tie2 signalling and modulates integrin adhesions. In HUVECs adhering to a collagen-coated dish, Tie2 diffusely localized at bottom surface of the cells. In clear contrast, Tie2 was found to be punctate and phosphorylated at cell–substratum contacts when the cells were attached to a collagen- and COMP–Ang1-coated dish (Supplementary Information, Fig. S7d, e), indicating the capability of ECM-anchored Ang1 to stimulate Tie2. HUVECs adhering to collagen- and COMP–Ang1-coated substratum exhibited enhanced vinculin accumulation at the most peripheral region of the cells, compared with the cells attached to collagen, as analysed by line-scanning of immunofluorescence intensity (Fig. 5b, c). Consistently, fewer stress fibres and more lamellipodia were observed in the presence of COMP–Ang1 (Supplementary Information, Fig. S7f). These data reveal that Ang1–Tie2 signalling at cell–substratum contacts induces FC formation.
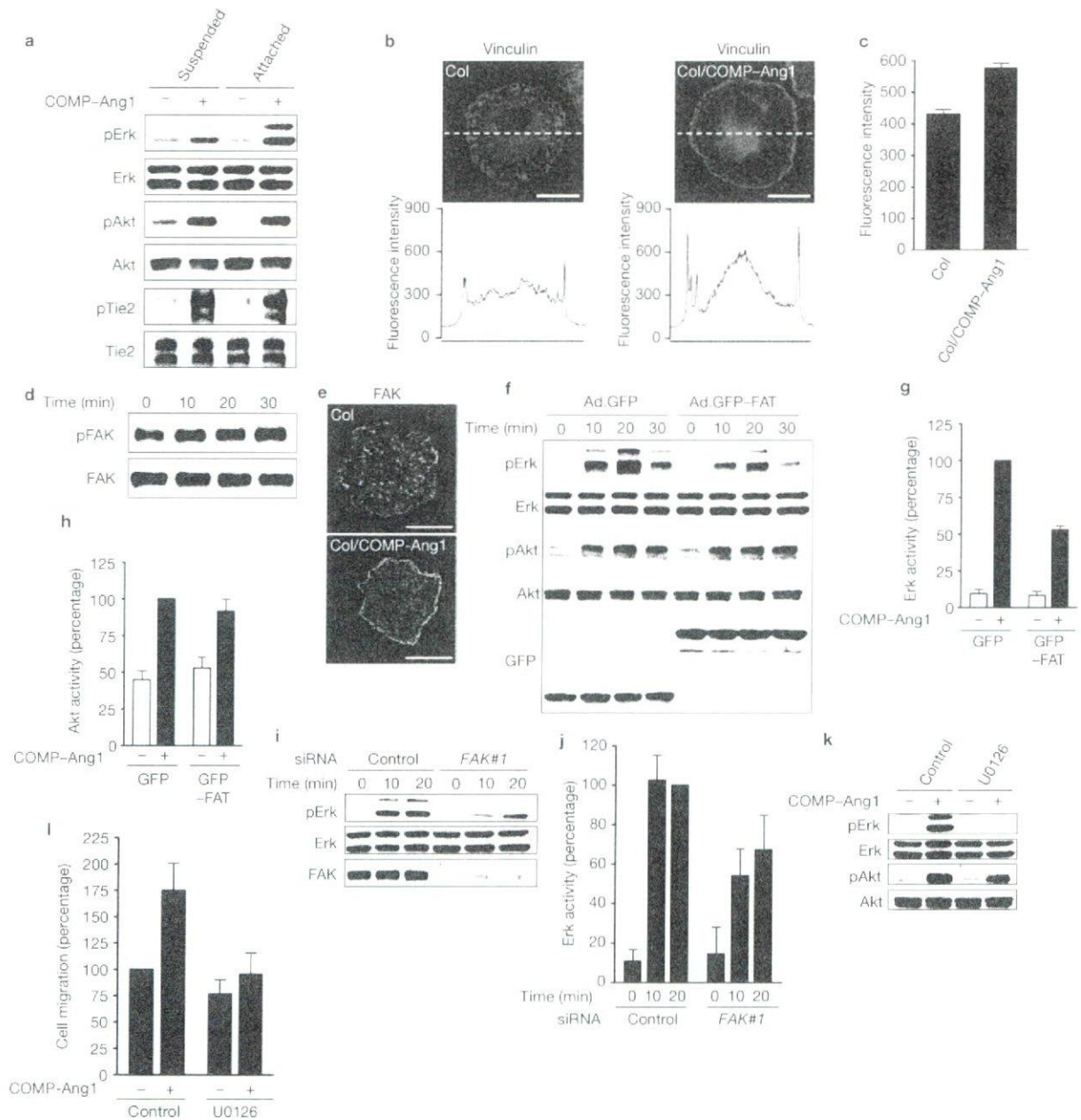
Figure 5 Activation of Erk by Tie2 at cell–substratum contacts partly depends upon FAK and is involved in endothelial cell migration. (a) Suspended HUVECs and cells adhered on a as described in Supplementary Methods. (b) HUVECs were placed on the COMP–Ang1–unbound collagen-coated dish (Col) or COMP–Ang1–bound collagen-coated dish (Col and COMP–Ang1) for 30 min, and immunostained with anti-vinculin antibody. Focal complexes were analysed by line intensity scan using MetaMorph 6.1 software (fluorescence intensity along the dotted line indicated, bottom panels). (c) Quantification of the Results of b. Values are expressed as means ± s.d. of fluorescence intensity relative to vinculin at the cell periphery (Col, n = 60; Col & COMP–Ang1, n = 66). (d) Sparse HUVECs starved for 6 h were stimulated with COMP–Ang1 for different times (min). Immunoprecipitates and cell lysate were subjected to western blot analysis with anti-phosphotyrosine (pFAK) and anti-FAK (FAK) antibodies, respectively. (e) Localization of FAK was examined similarly to b. (f) Sparse HUVECs plated on a collagen-coated dish were infected with adenovirus vector encoding either GFP or GFP–FAT as described in Supplementary Information, Methods. Cells stimulated with COMP–Ang1 for 20 min were analysed for Erk and Akt activation. (g, h) Phosphorylation of Erk (g) and Akt (h) in f was quantified. Values are expressed as means ± s.d. from five independent experiments. (i) Effect of knockdown of FAK on Erk activation was examined in control siRNA (control) or FAK siRNA-treated HUVECs (FAK No.1). (j) Quantification of the results of i. Values are expressed as means ± s.d. from 6 independent experiments. (k, l) MEK–Erk inhibition results in decreased migration of sparse HUVECs stimulated with COMP–Ang1. 20 μM U0126 (a MEK inhibitor) inhibits COMP–Ang1-induced Erk, but not Akt activation (k). Migration of HUVECs was analysed as described in Supplementary Methods (l). Values are expressed as the mean ± s.d. from 5 independent experiments. The scale bars represent 20 μm (b, e). Uncropped images of a, d, f, i, k are shown in Supplementary Information, Fig. S8.
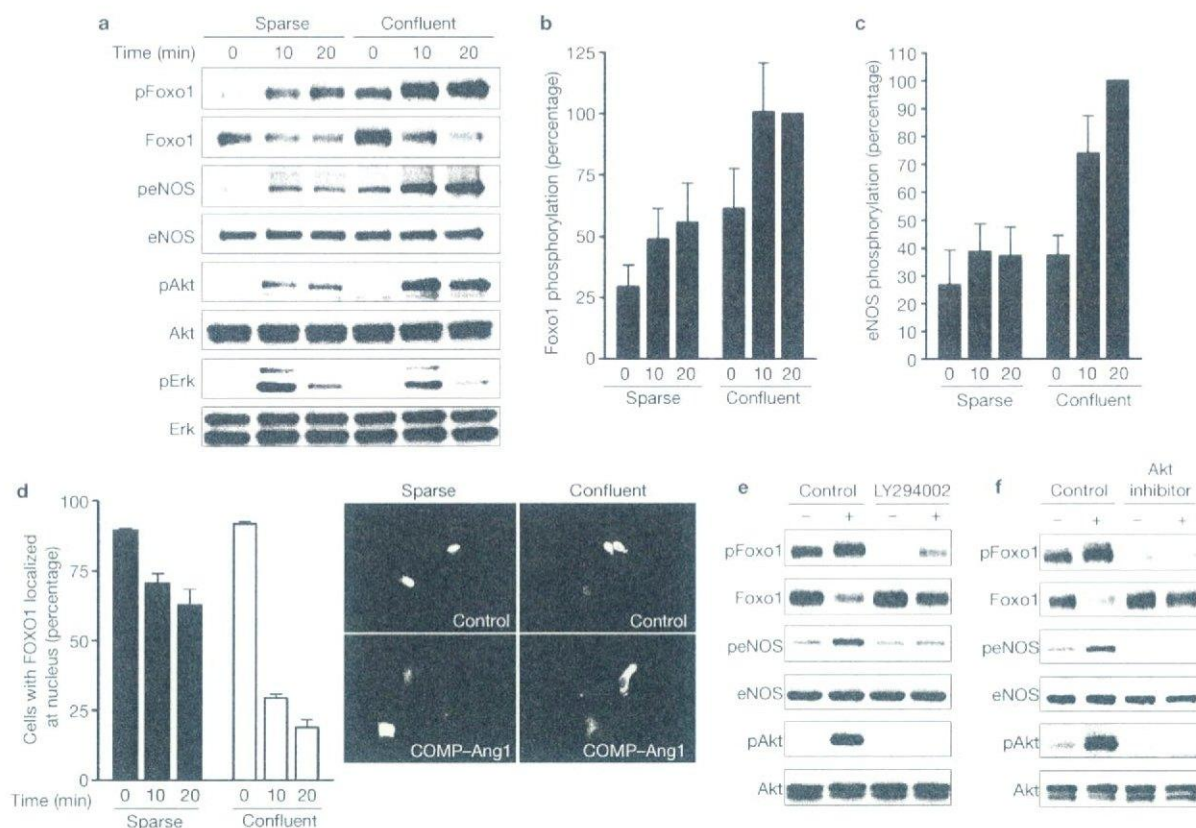
Figure 6 The presence of cell–cell contacts determines the preferential activation of Akt and subsequent phosphorylation of Foxo1 and eNOS. (a) Sparse and confluent HUVECs were starved and stimulated with COMP–Ang1. Cell lysates were analysed for phosphorylation of Foxo1, eNOS, Akt, and Erk. Note that Foxo1 and eNOS are more phosphorylated in the confluent cells than in the sparse cells. (b) COMP–Ang1–induced phosphorylation of Foxo1 observed in **a** was quantified. Foxo1 phosphorylation represents the ratio of phosphorylated Foxo1 to total Erk protein as a percentage of the ratio in the confluent cells stimulated for 20 min. Erk protein but not Foxo1 was used as normalization for protein loading, because anti-Foxo1 antibody does not recognize phosphorylated Foxo1. Values are expressed as means ± s.d. from seven independent experiments. (c) COMP–Ang1-induced phosphorylation of eNOS observed in **a** was quantified. eNOS phosphorylation represents the ratio of phosphorylated eNOS to total eNOS as a percentage of the ratio in the confluent cells stimulated for 20 min. Values are expressed as means ± s.d. from seven independent experiments. (d) Sparse and confluent HUVECs transfected with a plasmid encoding GFP–Foxo1 were starved for 6 h and stimulated with COMP–Ang1 for the time (min) as indicated. After fixation in methanol, the number of cells with GFP–Foxo1 localized at nucleus was counted and expressed as a percentage relative to total number of cells. At least 100 GFP-positive cells were scored for each treatment. Values are expressed as means ± s.d. from three independent experiments. Representative images of subcellular localization of GFP–Foxo1 in sparse (left) and confluent (right) cells are shown on the bottom. Upper and lower panels show the images in cells stimulated with vehicle or COMP–Ang1 for 20 min. (e, f) Confluent HUVECs were pre-treated with 20 µM LY294002 for 30 min (e) or 8 µM Akt inhibitor for 5 min (f) and subsequently stimulated with vehicle (–) or COMP–Ang1 (+) for 20 min. The effect of both inhibitors on COMP–Ang1-induced phosphorylation of Foxo1, eNOS, and Akt was examined. Uncropped images of **a**, **e**, and **f** are shown in Supplementary Information, Fig. S8.

Focal adhesion kinase (FAK) localizing at FCs and FAs mediates signalling by integrins and growth factor receptors to activate Erk[46,47]. Previously, it has been reported that Ang1 activates FAK to induce endothelial cell sprouting[13]. Thus, we tested the involvement of FAK in Erk activation downstream of cell–substratum contact-anchored Tie2 upon Ang1 stimulation. COMP–Ang1 induced tyrosine phosphorylation and accumulation of FAK to FCs in HUVECs (Fig. 5d and Supplementary Information, Fig. S7g) and increased the FAK-positive FC assembly as well as vinculin (Fig 5b, e). Consistent with the idea that the focal-adhesion-targeting domain of FAK (FAT) displaces FAK from FCs and FAs[36], overexpression of RFP-tagged FAT (RFP–FAT) perturbed the localization of FAK to FCs and FAs in HUVECs (Supplementary Information, Fig. S7h). Tie2 localization at peripheral cell–substratum contacts

upon COMP–Ang1 stimulation was not influenced by overexpression of FAT (Supplementary Information, Fig. S7i). We next investigated the effect of FAT on Tie2-mediated intracellular signalling. Overexpression of GFP-tagged FAT (GFP–FAT) significantly but not completely inhibited COMP–Ang1-induced Erk activation (Fig. 5f, g). In clear contrast, overexpression of FAT did not alter COMP–Ang1-induced Akt activation (Fig. 5f, h). Furthermore, depletion of FAK by siRNAs partly inhibited COMP–Ang1-induced Erk activation (Fig. 5i, j and Supplementary Information, Fig. S7j, k). Collectively, these results indicate that Erk activation by Tie2 anchored to cell–substratum contacts is ascribed partly to FAK.

Erk signalling is known to be involved in endothelial cell migration[18]. Thus, we examined the role of Erk in cell migration by Ang1–Tie2 at cell–substratum contacts. Cell motility was enhanced when HUVECs
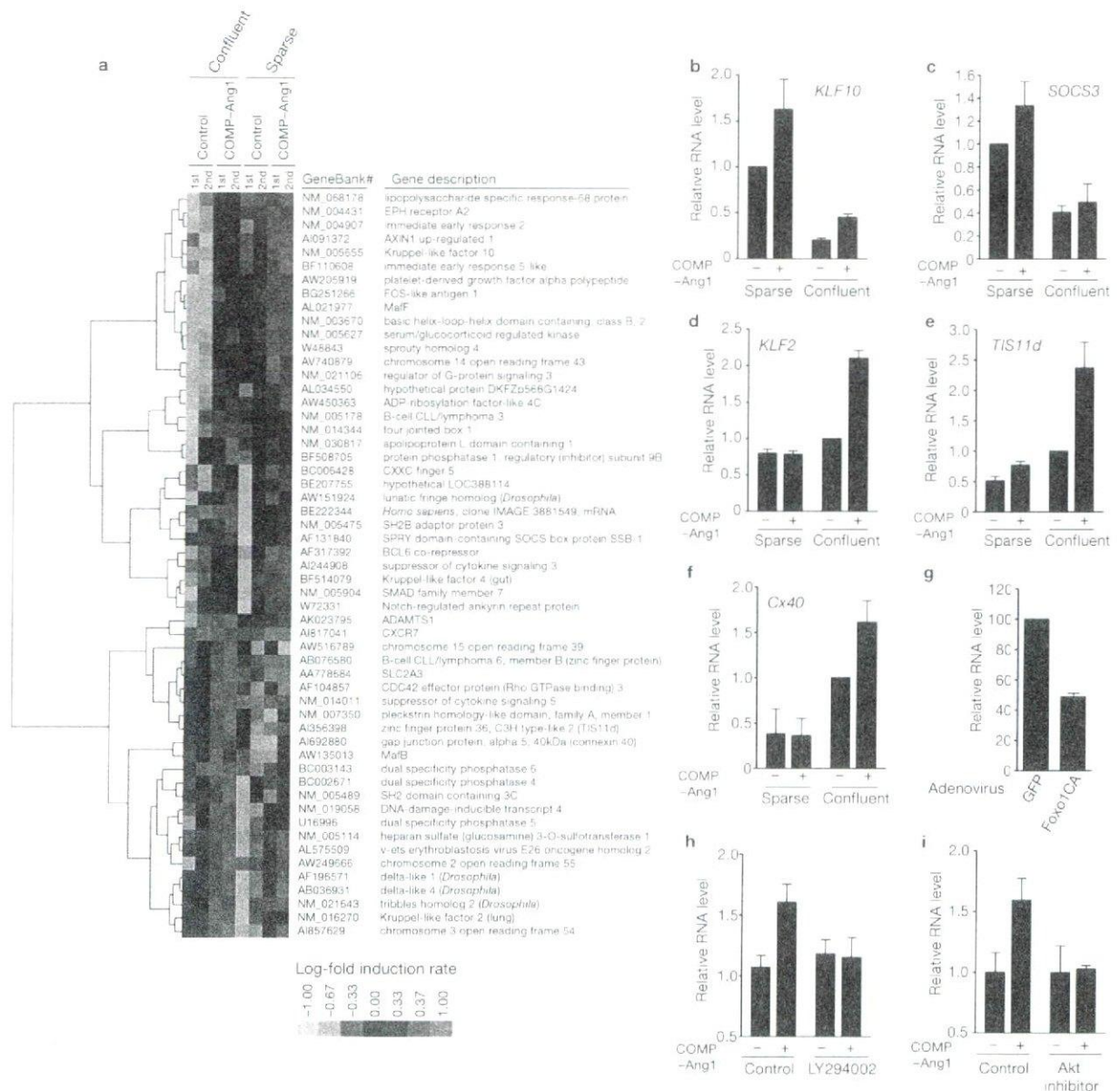
a

GeneBank#	Gene description
NM_068128	lipopolysaccharide specific response-68 protein
NM_004431	EPH receptor A2
NM_004907	immediate early response 2
AI091372	AXIN1 up-regulated 1
NM_005655	Kruppel-like factor 10
BF110608	immediate early response 5 like
AW205919	platelet-derived growth factor alpha polypeptide
BG251266	FOS-like antigen 1
AL021977	MafF
NM_003670	basic helix-loop-helix domain containing, class B, 2
NM_005627	serum/glucocorticoid regulated kinase
W45843	sprouty homolog 4
AV740879	chromosome 14 open reading frame 43
NM_021106	regulator of G-protein signaling 3
AL034550	hypothetical protein DKFZp566G1424
AW450363	ADP ribosylation factor-like 4C
NM_005178	B-cell CLL/lymphoma 3
NM_014344	four jointed box 1
NM_030817	apolipoprotein L, domain containing 1
BF508705	protein phosphatase 1, regulatory (inhibitor) subunit 9B
BC006428	CXXC finger 5
BE207755	hypothetical LOC388114
AW151924	lunatic fringe homolog (Drosophila)
BE222344	Homo sapiens, clone IMAGE:3881549, mRNA
NM_005475	SH2B adaptor protein 3
AF131840	SPRY domain-containing SOCS box protein SSB-1
AF317392	BCL6 co-repressor
AI244908	suppressor of cytokine signaling 3
BF514079	Kruppel-like factor 4 (gut)
NM_005904	SMAD family member 7
W72331	Notch-regulated ankyrin repeat protein
AK023795	ADAMTS1
AI817041	CXCR7
AW516789	chromosome 15 open reading frame 39
AB076580	B-cell CLL/lymphoma 6, member B (zinc finger protein)
AA778684	SLC2A3
AF104857	CDC42 effector protein (Rho GTPase binding) 3
NM_014011	suppressor of cytokine signaling 5
NM_007350	pleckstrin homology-like domain, family A, member 1
AI356398	zinc finger protein 36, C3H type-like 2 (TIS11d)
AI692880	gap junction protein, alpha 5, 40kDa (connexin 40)
AW135013	MafB
BC003143	dual specificity phosphatase 6
BC002671	dual specificity phosphatase 4
NM_005489	SH2 domain containing 3C
NM_019058	DNA-damage-inducible transcript 4
U16996	dual specificity phosphatase 5
NM_005114	heparan sulfate (glucosamine) 3-O-sulfotransferase 1
AL575509	v-ets erythroblastosis virus E26 oncogene homolog 2
AW249566	chromosome 2 open reading frame 55
AF196571	delta-like 1 (Drosophila)
AB036931	delta-like 4 (Drosophila)
NM_021643	tribbles homolog 2 (Drosophila)
NM_016270	Kruppel-like factor 2 (lung)
AI857629	chromosome 3 open reading frame 54

Log-fold induction rate

−1.00 −0.67 −0.33 0.00 0.33 0.37 1.00

Figure 7 Ang1 stimulation leads to a distinct pattern of gene expression in HUVECs in the presence or absence of cell–cell contacts. (**a**) Total RNA was purified from confluent and sparse HUVECs stimulated with vehicle (control) or COMP–Ang1 for 1 h, and subjected to Affymetrix microarray analysis, as described in Methods. Genes corresponding to the criteria described in Methods were subjected to the cluster analysis. The results from two independent microarray analyses are displayed. Red and green represent higher and lower expression than the median for that particular gene, respectively. Color intensity is related to the difference with the median (black). (**b–f**) Total RNA was purified from confluent and sparse HUVECs stimulated with vehicle (−) or COMP–Ang1 (+) for 1 h, and expression levels of KLF10 (**b**), SOCS3 (**c**), KLF2 (**d**), TIS11d (**e**) and Cx40 (**f**) were analysed by real-time RT–PCR analysis as described in Supplementary Information, Methods. Bar graphs show relative RNA levels of each gene normalized to GAPDH levels. RNA levels are expressed relative to that in sparse (**b**, **c**) or confluent (**d–f**) cells stimulated with vehicle. Values are expressed as means ± s.d. from more than three independent experiments. (**g**) Total RNA was isolated from confluent HUVECs infected with adenovirus vectors encoding either GFP (GFP) or a constitutively active mutant of Foxo1 (Foxo1CA). Expression levels of Cx40 were analysed as described for **f**, and expressed as a percentage relative to that in cells infected with GFP-encoding adenovirus vector. (**h**) Confluent HUVECs were stimulated with COMP–Ang1 in the presence (LY294002) or absence (control) of LY294002 as described in the legend of Fig. 6e. Expression levels of Cx40 were analysed as described for **f**. Data are means ± s.d. of triplicate samples, and similar results were obtained in three independent experiments. (**i**) Confluent HUVECs were stimulated with COMP–Ang1 in the presence (Akt inhibitor) or absence (control) of Akt inhibitor as described in the legend of Fig. 6f. Expression levels of Cx40 were analysed and expressed as described for **h**.

were placed on collagen- and COMP–Ang1-coated transwell filters, compared with cells adhering to collagen-coated filters. This enhanced cell motility was cancelled by inhibiting Erk using U0126, a MEK inhibitor (Fig. 5k, l). These findings suggest that Ang1–Tie2 at cell–substratum contacts regulates endothelial cell migration through the Erk signalling pathway.

− 126 −

Presence of cell–cell contacts
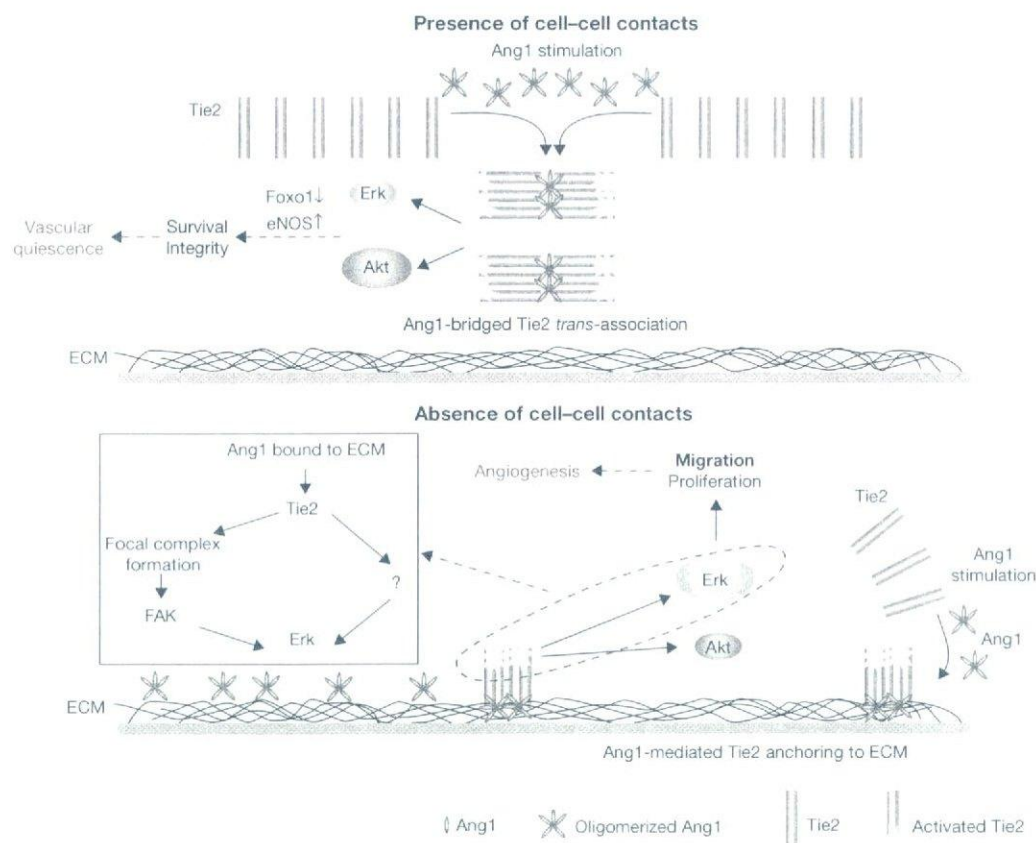
Absence of cell–cell contacts

Figure 8 Schematic representation of a proposed model for how Ang1–Tie2 signalling is involved in both vascular quiescence and angiogenesis. (Upper panel) Under confluent conditions, oligomerized Ang1 bridges Tie2 at cell–cell contacts, resulting in formation of *trans*-association of Tie2. *Trans*-associated Tie2 at cell–cell contacts preferentially activates Akt–Foxo1 and Akt–eNOS signalling pathways, which may contribute to maintenance of vascular quiescence by enhancing endothelial survival and integrity (dashed arrows). (Lower panel) In the absence of cell–cell contacts, Tie2 forms a complex with ECM-bound Ang1 at cell–substratum contacts, which is different from focal adhesions, focal complexes and fibrillar adhesion. Ang1–Tie2 anchored to cell–substratum contacts preferentially activates the Erk pathway by inducing FAK-positive focal complex assembly. Ang1, therefore, seems to implicate FAK partly in the activation of Erk. This preferential activation of the Erk pathway induced by Ang1–Tie2 anchored to cell–substratum contacts may contribute to endothelial cell migration and proliferation, thereby promoting angiogenesis (dashed arrows). FC and ECM indicate focal complex and extracellular matrix, respectively.

The presence of cell–cell contacts determines preferential activation of Akt by Ang1 and subsequent phosphorylation of eNOS and Foxo1

Akt phosphorylates the forkhead transcription factor Foxo1 and endothelial nitric oxide synthase (eNOS), which play critical roles in endothelial functions[39,40]. To investigate the biological consequence of preferential activation of Akt by *trans*-associated Tie2, we examined Ang1-induced phosphorylation of Foxo1 and eNOS in the absence and presence of cell–cell contacts. Endothelial cell–cell contacts significantly enhanced COMP–Ang1-induced phosphorylation of Foxo1 and eNOS in HUVECs (Fig. 6a–c). Akt-dependent phosphorylation negatively regulates transcriptional activity of Foxo1 by promoting its nuclear exclusion. Consistently, nuclear export of Foxo1 by COMP–Ang1 was more prominent in confluent HUVECs than in sparse cells (Fig. 6d). Phosphatidylinositol-3 kinase (PI3K) inhibitor, LY294002, and Akt inhibitor impeded COMP–Ang1-induced phosphorylation of Foxo1 and eNOS (Fig. 6e, f). These findings indicate that phosphorylation of Foxo1 and eNOS mediated by PI3K–Akt are preferentially induced by *trans*-associated Tie2 compared to substratum-anchored Tie2.

Distinct gene expression profile in HUVECs upon Ang1 stimulation in the presence or absence of cell–cell contacts

To further clarify the consequence of Tie2 activation at cell–cell contacts and at cell–substratum contacts, we employed DNA microarray analyses. We carried out a global survey of mRNA in either confluent or sparse HUVECs upon COMP–Ang1 stimulation for 1 h. There was a striking difference in the induction of genes between confluent and sparse conditions (Fig. 7a). To confirm the microarray data, expression levels of several genes selectively induced under either sparse or confluent conditions were examined by quantitative real-time PCR analysis. Both basal expression and induction of *Krüppel-like factor* (*KLF*) *10* and *suppressor of cytokine signaling 3* (*SOCS3*) were greater in sparse cells than in confluent cells (Fig. 7b, c). In contrast,

KLF2, zinc finger protein 36, C3H type 2 (TIS11d), and connexin40 (Cx40) were induced by COMP–Ang1 selectively in confluent cells (Fig. 7d, e, f). Cx40, the product of which is involved in intercellular communication, is known to be repressed by Foxo1 in endothelial cells.[39] Indeed, overexpression of a constitutively active mutant of Foxo1 decreased Cx40 expression (Fig. 7g). Thus, we investigated whether a PI3K–Akt–Foxo1 signal axis is involved in COMP–Ang1-induced Cx40 expression. LY294002 and Akt inhibitor prevented COMP–Ang1-induced Cx40 induction in confluent cells (Fig. 7h, i). Collectively, these microarray analyses and real-time PCR validation clearly demonstrate a difference in induction of gene expression by Ang1 in the presence or absence of cell–cell contacts, and indicate that trans-associated Tie2 at cell–cell contacts regulates Foxo1-dependent gene expression through preferential activation of Akt.

DISCUSSION

Localization of Tie2 upon Ang1 stimulation depends upon the presence or absence of cell–cell contacts (Figs 1a, 3a). Tie2 localization at cell–cell contacts appears to be due to Ang1-bridged Tie2 trans-association. Tie2 activation at cell–cell contacts resulted in preferential activation of Akt, which in turn led to inhibition of Foxo1-mediated gene regulation and phosphorylation of eNOS. The Akt–Foxo1 pathway is known to be involved in Ang1-induced endothelial cell survival and blood vessel stability.[39] It has been also reported that the Akt–eNOS pathway is required for vascular maturation.[10] Thus, trans-associated Tie2 may contribute to maintenance of vascular quiescence through the Akt–Foxo1 and Akt–eNOS signalling pathways.

Ang1 also locates Tie2 to cell–substratum contacts that are different from FCs, FAs and FBs and preferentially activates Erk in the absence of cell–cell contacts. This Tie2 localization was resistant to detergent[27,28], indicating Tie2 is anchored to cell–substratum contacts. Moreover, Ang1 could bind to ECM such as fibronectin and collagen, as previously reported[11,42]. Upon being anchored to ECM by Ang1, Tie2 activated Erk partly through FAK. Formation of the Ang1–Tie2 complex at cell–substratum contacts accelerated FC formation (Fig. 5b, e), and probably vice versa, resulting in the implicating FAK in Ang1-induced Erk activation in isolated cells. This notion is consistent with recent reports revealing a role for FAK in vascular development[43,44].

During angiogenesis, endothelial cells sprouting from the preexisting blood vessels lose cell–cell adhesion and need to proliferate and migrate to form neovasculature. Erk is responsible for endothelial proliferation and migration during angiogenesis[38,45]. Inhibition of Erk resulted in decreased migration by substratum-anchored Ang1. As several lines of evidence suggest that Tie2 signalling mediates pathological and physiological angiogenesis[14,15,17-20], Ang1–Tie2–ECM complexes at cell–substratum contacts may accelerate angiogenesis by promoting proliferation and migration of isolated endothelial cells. However, regulation of angiogenesis by Ang1–Tie2 might be more complex, since it has been reported that Tie2 is expressed in stalk cells, but not in tip cells, which proliferate and migrate during angiogenesis[46]. Thus, further investigation is required to resolve this mechanism.

We propose that trans-associated Tie2 bridged by Ang1 and cell–substratum contact-anchored Tie2 by Ang1 might be preferable for vascular quiescence and for angiogenesis via Akt and Erk activation, respectively (Fig. 8). □

Note added in proof: a related manuscript by Saharinen et al. (Nature Cell Biol. **10**, 527–537; doi:10.1038/ncb1715; 2008) is also published in this issue.

METHODS

Immunocytochemistry and fluorescence imaging. HUVECs and CHO cells grown on a collagen-coated glass-base dish (Asahi Techno Glass Corporation, Chiba, Japan) were transfected with expression plasmids encoding Tie2–GFP, Tie2Δcyto–GFP, Tie2Δcyto–HA, RFP–Crk, GFP–tensin and RFP–FAT as indicated in the figures. HUVECs starved for 3 h in medium 199 containing 0.5% BSA and CHO cells in Dulbecco's modified Eagle's medium (DMEM)/F12 nutrient mixture (Sigma-Aldrich, St. Louis, MO) were stimulated for the time periods as indicated in the figures. After stimulation, the cells were fixed in PBS containing 2% formaldehyde for 30 min at 4 °C, washed with PBS, and permeabilized with 0.05% Triton X-100 for 30 min at 4 °C. To examine the detergent insolubility of Tie2–GFP anchoring to the substratum, the cells were washed with PBS, and extracted in 0.5% Triton X-100 in cytoskeleton stabilizing buffer containing 10 mM PIPES at pH 6.8, 300 mM sucrose, 100 mM NaCl, 3 mM MgCl, 1 mM EGTA and 1 × protease inhibitor cocktail (Roche Applied Science, Indianapolis, IN) for 3 min at room temperature (RT). After washing with PBS, the cells were fixed with 2% formaldehyde in PBS for 30 min at 4 °C. Cells were blocked with PBS containing 4% BSA for 1 h at RT and immunostained with anti-Tie2, anti-VE-cadherin, anti-HA, anti-FLAG, anti-vinculin, anti-α5 integrin, anti-β3 integrin, anti-PECAM-1, anti-VASP, anti-talin, anti-fibronectin, anti-phosphoTie2, and anti-FAK antibodies for 1 h at RT and with rhodamine-phalloidin for 20 min at RT. Protein reacting with antibody was visualized with species-matched Alexa 488- or Alexa 546-labelled secondary antibodies. Fluorescence images of GFP, RFP, rhodamine, Alexa 488 and Alexa 546 were recorded with an Olympus IX-81 inverted fluorescence microscope (Olympus Corporation, Tokyo, Japan) with a cooled CCD camera CoolSNAP-HQ (Roper Scientific, Tucson, AZ), and appropriate filter sets for GFP, Alexa 488 and Alexa 546, and with a FluoView FV1000 confocal microscope (Olympus Corporation) with a 60x oil immersion objective lens. HUVECs and CHO cells transfected with plasmids expressing fluorescently tagged proteins (GFP, HcRed, and RFP) were time-lapse imaged on an Olympus IX-81 inverted fluorescence microscope as described previously[17,18].

In vitro Ang1-bridged Tie2 association assay. To produce recombinant sTie2–HA protein (extracellular domain of Tie2 tagged with HA), 293F cells were transfected with pcDNA3.1 sTie2–HA vector, and cultured in Free Style 293 expression media for 7 days. sTie2–HA protein secreted into the medium was collected every 2 days, and incubated with ProBond resin (Invitrogen Corp., Carlsbad, CA) overnight at 4 °C. sTie2–HA protein bound to the beads was eluted with 500 mM imidazole, concentrated with Amicon Centriplus (Millipore, Billerica, MA), and buffer exchanged into PBS by dialysis.

Ang1-bridged Tie2 association was analysed as described in Supplementary Information Fig. S3a. Initially, protein G sepharose beads (GE Healthcare Life Science, Piscataway, NJ) were incubated with 0.1 μg of Fc, sTie1–Fc or sTie2–Fc protein in binding buffer (50 mM Tris-HCl at pH 7.5, 100 mM NaCl, 0.02% Triton X-100) for 2 h at 4 °C, washed three times with binding buffer, and incubated with 1 μg of Ang1 or its variants (COMP–Ang1, GCN4–Ang1 and MAT–Ang1) for 2 h at 4 °C. The beads were extensively washed with binding buffer four times, and subsequently incubated with 3 μg of sTie2–HA protein for 2 h at 4 °C. After washing, the precipitates were subjected to Western blot analysis with anti-Flag and anti-HA antibodies to quantify the co-precipitated Ang1 and its variants and sTie2–HA protein, respectively. Proteins reacting with primary antibodies were visualized by the ECL system (GE Healthcare Life Science) for detecting peroxidase-conjugated secondary antibodies and analysed with an LAS-1000 system (Fuji Film, Tokyo, Japan).

Cell aggregation and in vivo Tie2 trans-association assays. Suspension 293F cells transfected with the plasmids expressing GFP, Tie2–GFP, Tie2Δcyto–GFP, Tie2KD–GFP, or VEGFR2 plus IRES-driven GFP were suspended in Free Style 293 expression media and placed on 6 well-plates in a density of 5.0 × 10^{5} cells per well (1 ml per well). Then, the cells were agitated for 4 h using a gyratory shaker in the presence of vehicle, Ang1, COMP–Ang1 or VEGF. After the incubation, the phase-contrast and the fluorescence images were recorded by Olympus IX-81 inverted fluorescence microscope. The differential interference contrast (DIC) and the fluorescence images were also obtained with a FluoView

FV1000 confocal microscope. The numbers of cell aggregates including more than 4 cells were counted in, at least, 10 different fields. The size of cell aggregates was measured using MetaMorph 6.1 software.

For the *in vivo* Tie2 *trans*-association assay, 293F cells transfected with the vectors encoding either GFP, Tie2Δcyto–GFP, or Tie2Δcyto–HA were washed and resuspended in DMEM in a density of 10^6 cells per ml. The cells expressing Tie2Δcyto–HA were mixed with either those expressing Tie2Δcyto–GFP or those expressing GFP in a 6 well-plate (2×10^6 cells well^{-1}). The cell suspensions were agitated for 1 h in the presence or absence of 400 ng ml^{-1} COMP-Ang1. After the incubation, the cells were collected in a 15 ml-conical tube, washed with ice-cold PBS and lysed at 4°C in lysis buffer containing 50 mM Tris-HCl at pH 7.5, 150 mM NaCl, 0.5% Triton X-100 and 1 x protease inhibitor cocktail. BaF–Tie2Δcyto–HA cells (1.5 x 10^6 cells) were also mixed with either BaF3 cells (1.5 x 10^6 cells) or BaF–Tie2Δcyto–GFP cells (1.5 x 10^6 cells) in RPMI1640 (Nissui, Tokyo, Japan) supplemented with 2 ng ml^{-1} murine IL3, and stimulated with or without 400 ng ml^{-1} COMP-Ang1 for 5 h. After the incubation, the cells were washed with ice-cold PBS and lysed as described above. Precleared cell lysates were subjected to immunoprecipitaion with anti-GFP antibody followed by immunoblot analysis with anti-HA antibody.

Microarray analysis. Confluent and sparse HUVECs on a collagen-coated dish were starved in HuMedia-EB2 medium (Kurabo, Kurashiki, Japan) containing 0.5% fetal calf serum (FCS) for 15 h, and stimulated with vehicle or COMP-Ang1 (200 ng ml^{-1}) for 1 h. After the stimulation, total RNAs were purified from the pooled RNA of triplicate samples using Trizol reagent (Invitrogen Corp.) and reverse-transcribed to cDNAs. Biotin-labelled RNAs derived from cDNAs were fragmented according to the manufacturer's instructions (Affymetrix, Santa Clara, CA). Labelled cRNA probes were hybridized to Affymerix U133plus 2.0 array (Affymetrix). The microarray data scanned through an Affymetrix GeneChip scanner 3000 7G were globally normalized by Affymetrix Microarray Suite 5.0 software and were scaled to a target intensity of 100. Microarray analysis was performed in duplicate from independent RNA preparations. Data were analysed according to the minimum information about a microarray experiment (MIAME) rule. To identify the genes regulated by Ang1–Tie2 signal, we picked up the genes which fulfill the two criteria: (1) the hybridization signal after COMP-Ang1 stimulation was higher than 80 in duplicate experiments and (2) the induction was greater than 1.5-fold under either confluent or sparse conditions upon COMP-Ang1 stimulation in duplicate experiments. The genes that conformed to the two criteria were further clustered on the basis of similar regulation patterns using Gene cluster (created by M. B. Eisen, University od California, Berkeley, CA) and Java Tree View software according to the manual on the default settings. The complete microarray data sets are available from the Gene Expression Omnibus (GSE9677).

Note: Supplementary Information is available on the Nature Cell Biology website.

AUTHOR CONTRIBUTIONS
S. F. and N. M. designed and wrote the paper. S. F. performed the all cell biological and biochemical analysis. K. S. and K. N. helped with the experiments performed by S. F. T. M. and T. K. performed microarray analyses. M. S. and N. T. helped with VEGF related and Tie2–BaF experiments. H. Z. K. and G. Y. K. prepared several forms of recombinant Ang1.

1. Yancopoulos, G. D. *et al.* Vascular-specific growth factors and blood vessel formation. *Nature* **407**, 242–248 (2000).
2. Mammoto, T. *et al.* Angiopoietin-1 requires p190RhoGAP to protect against vascular leakage *in vivo*. *J. Biol. Chem.* **282**, 23910–23918 (2007).
3. Jho, D. *et al.* Angiopoietin-1 opposes VEGF-induced increase in endothelial permeability by inhibiting TRPC1-dependent Ca2 influx. *Circ. Res.* **96**, 1282–1290 (2005).
4. Brindle, N. P., Saharinen, P. & Alitalo, K. Signaling and functions of angiopoietin-1 in vascular protection. *Circ. Res.* **98**, 1014–1023 (2006).
5. Baffert, F., Le, T., Thurston, G. & McDonald, D. M. Angiopoietin-1 decreases plasma leakage by reducing number and size of endothelial gaps in venules. *Am. J. Physiol. Heart Circ. Physiol.* **290**, H107-H118 (2005).
6. Gamble, J. R. *et al.* Angiopoietin-1 is an antipermeability and anti-inflammatory agent *in vitro* and targets cell junctions. *Circ. Res.* **87**, 603–607 (2000).
7. Cho, C. H. *et al.* Designed angiopoietin-1 variant, COMP-Ang1, protects against radiation-induced endothelial cell apoptosis. *Proc. Natl Acad. Sci.USA* **101**, 5553–5558 (2004).
8. Kwak, H. J., So, J. N., Lee, S. J., Kim, I. & Koh, G. Y. Angiopoietin-1 is an apoptosis survival factor for endothelial cells. *FEBS Lett.* **448**, 249–253 (1999).
9. Papapetropoulos, A. *et al.* Angiopoietin-1 inhibits endothelial cell apoptosis via the Akt/Survivin pathway. *J. Biol. Chem.* **275**, 9102–9105 (2000).
10. Thurston, G. *et al.* Angiopoietin-1 protects the adult vasculature against plasma leakage. *Nature Med.* **6**, 460–463 (2000).
11. Thurston, G. *et al.* Leakage-resistant blood vessels in mice transgenically overexpressing angiopoietin-1. *Science* **286**, 2511–2514 (1999).
12. Master, Z. *et al.* Dok-R plays a pivotal role in angiopoietin-1 dependent cell migration through recruitment and activation of Pak. *EMBO J.* **20**, 5919–5928 (2001).
13. Kim, I. *et al.* Angiopoietin-1 induces endothelial cell sprouting through the activation of focal adhesion kinase and plasmin secretion. *Circ. Res.* **86**, 952–959 (2000).
14. Cho, C. H. *et al.* COMP-Ang1: A designed angiopoietin-1 variant with nonleaky angiogenic activity. *Proc. Natl Acad. Sci. USA* **101**, 5547–5552 (2004).
15. Asahara, T. *et al.* Tie2 receptor ligands, angiopoietin-1 and angiopoietin-2, modulate VEGF-induced postnatal neovascularization. *Circ. Res.* **83**, 233–240 (1998).
16. Yoon, M. J. *et al.* Localization of Tie2 and phospholipase D in endothelial caveolae is involved in angiopoietin-1-induced MEK/ERK phosphorylation and migration in endothelial cells. *Biochem. Biophys. Res. Commun.* **308**, 101–105 (2003).
17. Lin, P. *et al.* Inhibition of tumor angiogenesis using a soluble receptor establishes a role for Tie2 in pathologic vascular growth. *J. Clin. Invest.* **100**, 2072–2078 (1997).
18. Lin, P. *et al.* Antiangiogenic gene therapy targeting the endothelium-specific receptor tyrosine kinase Tie2. *Proc. Natl Acad. Sci. USA* **95**, 8829–8834 (1998).
19. Peters, K. G. *et al.* Functional significance of Tie2 signaling in the adult vasculature. *Recent Prog. Horm. Res.* **59**, 51–71 (2004).
20. Wong, A. L. *et al.* Tie2 expression and phosphorylation in angiogenic and quiescent adult tissues. *Circ. Res.* **81**, 567–574 (1997).
21. Carmeliet, P. *et al.* Targeted deficiency or cytosolic truncation of the VE-cadherin gene in mice impairs VEGF-mediated endothelial survival and angiogenesis. *Cell* **98**, 147–157 (1999).
22. Zanetti, A. *et al.* Vascular endothelial growth factor induces SHC association with vascular endothelial cadherin: a potential feedback mechanism to control vascular endothelial growth factor receptor 2 signaling. *Arterioscler. Thromb. Vasc. Biol.* **22**, 617–622 (2002).
23. Lampugnani, M. G., Orsenigo, F., Gagliani, M. C., Tacchetti, C. & Dejana, E. Vascular endothelial cadherin controls VEGFR-2 internalization and signaling from intracellular compartments. *J. Cell Biol.* **174**, 593–604 (2006).
24. Zaidel-Bar, R., Cohen, M., Addadi, L. & Geiger, B. Hierarchical assembly of cell-matrix adhesion complexes. *Biochem. Soc. Trans.* **32**, 416–420 (2004).
25. Geiger, B., Bershadsky, A., Pankov, R. & Yamada, K. M. Transmembrane crosstalk between the extracellular matrix--cytoskeleton crosstalk. *Nature Rev. Mol. Cell Biol* **2**, 793–805 (2001).
26. Cascone, I., Napione, L., Maniero, F., Serini, G. & Bussolino, F. Stable interaction between aβ1 integrin and Tie2 tyrosine kinase receptor regulates endothelial cell response to Ang-1. *J. Cell Biol.* **170**, 993–1004 (2005).
27. Wulfkuhle, J. D. *et al.* Domain analysis of supervillin, an F-actin bundling plasma membrane protein with functional nuclear localization signals. *J. Cell Sci.* **112**, 2125–2136 (1999).
28. Adams, C. L., Nelson, W. J. & Smith, S. J. Quantitative analysis of cadherin-catenin-actin reorganization during development of cell-cell adhesion. *J. Cell Biol.* **135**, 1899–1911 (1996).
29. Kim, I. *et al.* Angiopoietin-1 regulates endothelial cell survival through the phosphatidylinositol 3'-Kinase/Akt signal transduction pathway. *Circ. Res.* **86**, 24–29 (2000).
30. Kanda, S., Miyata, Y., Mochizuki, Y., Matsuyama, T. & Kanetake, H. Angiopoietin 1 is mitogenic for cultured endothelial cells. *Cancer Res.* **65**, 6820–6827 (2005).
31. Teichert-Kuliszewska, K. *et al.* Biological action of angiopoietin-2 in a fibrin matrix model of angiogenesis is associated with activation of Tie2. *Cardiovasc. Res.* **49**, 659–670 (2001).
32. Weber, C. C. *et al.* Effects of protein and gene transfer of the angiopoietin-1 fibrinogen-like receptor-binding domain on endothelial and vessel organization. *J. Biol. Chem.* **280**, 22445–22453 (2005).

ARTICLES

33. Dallabrida, S. M., Ismail, N., Oberle, J. R., Himes, B. E. & Rupnick, M. A. Angiopoietin-1 promotes cardiac and skeletal myocyte survival through integrins. *Circ. Res.* **96**, e8-24 (2005).

34. Aplin, A. E., Short, S. M. & Juliano, R. L. Anchorage-dependent regulation of the mitogen-activated protein kinase cascade by growth factors is supported by a variety of integrin α chains. *J. Biol. Chem.* **274**, 31223–31228 (1999).

35. Short, S. M., Talbott, G. A. & Juliano, R. L. Integrin-mediated signaling events in human endothelial cells. *Mol. Biol. Cell* **9**, 1969–1980 (1998).

36. Schlaepfer, D. D. & Mitra, S. K. Multiple connections link FAK to cell motility and invasion. *Curr. Opin. Genet. Dev.* **14**, 92–101 (2004).

37. Parsons, J. T. Focal adhesion kinase: the first ten years. *J. Cell Sci.* **116**, 1409–1416 (2003).

38. Eliceiri, B. P., Klemke, R., Stromblad, S., & Cheresh, D. A. Integrin αV β3 requirement for sustained mitogen-activated protein kinase activity during angiogenesis. *J. Cell Biol.* **140**, 1255–1263 (1998).

39. Daly, C. *et al.* Angiopoietin-1 modulates endothelial cell function and gene expression via the transcription factor FKHR (FOXO1). *Genes Dev.* **18**, 1060–1071 (2004).

40. Chen, J. *et al.* Akt1 regulates pathological angiogenesis, vascular maturation and permeability in vivo. *Nature Med.* **11**, 1188–1196 (2005).

41. Xu, Y. & Yu, Q. Angiopoietin-1, unlike angiopoietin-2, is incorporated into the extracellular matrix via its linker peptide region. *J. Biol. Chem.* **276**, 34990–34998 (2001).

42. Carlson, T. R., Feng, Y., Maisonpierre, P. C., Mrksich, M. & Morla, A. O. Direct cell adhesion to the angiopoietins mediated by integrins. *J. Biol. Chem.* **276**, 26516–26525 (2001).

43. Braren, R. *et al.* Endothelial FAK is essential for vascular network stability, cell survival, and lamellipodial formation. *J. Cell Biol.* **172**, 151–162 (2006).

44. Shen, T. L. *et al.* Conditional knockout of focal adhesion kinase in endothelial cells reveals its role in angiogenesis and vascular development in late embryogenesis. *J. Cell Biol.* **169**, 941–952 (2005).

45. Meadows, K. N., Bryant, P. & Pumiglia, K. Vascular endothelial growth factor induction of the angiogenic phenotype requires Ras activation. *J. Biol. Chem.* **276**, 49289–49298 (2001).

46. Yana, I. *et al.* Crosstalk between neovessels and mural cells directs the site-specific expression of MT1-MMP to endothelial tip cells. *J. Cell Sci.* **120**, 1607–1614 (2007).

47. Nagashima, K. *et al.* Adaptor protein Crk is required for ephrin-B1-induced membrane ruffling and focal complex assembly of human aortic endothelial cells. *Mol. Biol. Cell* **13**, 4231–4242 (2002).

48. Sakurai, A. *et al.* MAGI-1 is required for Rap1 activation upon cell-cell contact and for enhancement of vascular endothelial cadherin-mediated cell adhesion. *Mol. Biol. Cell* **17**, 966–976 (2006).

Angiopoietin-1 alters tumor growth by stabilizing blood vessels or by promoting angiogenesis

Naoyuki Satoh, Yoshihiro Yamada, Yumi Kinugasa and Nobuyuki Takakura[1]

Department of Signal Transduction, Research Institute for Microbial Diseases, Osaka University, 3-1 Yamadaoka, Suita-shi, Osaka 565-0871, Japan

The maturation of blood vessels requires mural cell adhesion to endothelial cells. Angiopoietin-1 (Ang1), a ligand for Tie2 receptor expressed on endothelial cells, plays a critical role in cell adhesion between mural cells and endothelial cells and in endothelial cell sprouting from preexisting vessels in the absence of mural cells. Much information has been amassed on the Tie2–Ang1 system in physiological blood vessel formation during embryogenesis; however, the role of Ang1 in the tumor environment and its interaction with mural cells has not been well documented. Here we studied how Ang1 regulates maturation of blood vessels using the human colon cancer cell line HT29 and the human prostate cancer cell line PC3, and studied how Ang1 affects tumor growth. In a xenograft tumor model using female nude mice, we found that Ang1 enhanced angiogenesis and resulted in tumor growth in the case of PC3 tumors but suppressed tumor growth in the case of HT29 tumors. In PC3 tumors, the number of mural cells adhering to endothelial cells was less than that in HT29 tumors. Ang1 induced sprouting angiogenesis in PC3 tumors although there was little maturation of blood vessels. On the other hand, there was abundant mural cell adhesion to endothelial cells in HT29 tumors and Ang1 did not induce angiogenesis. These results suggest that Ang1 alters tumor growth in a manner that is dependent on the adhesion of mural cells and their localization in the tumor environment. (*Cancer Sci* 2008; 99: 2373–2379)

B lood vessel formation commences by assembly and tube formation of endothelial cells (EC), or EC progenitors. This process is termed vasculogenesis and is followed by angiogenesis, which results in the emergence of new vessels through the sprouting and elongation from, or the remodeling of, preexisting vessels.[1] In both processes, the structural stability of the tube made of EC is derived from mural cells (MC), such as smooth muscle cells and pericytes, that are recruited around EC forming the tube and adhere to them. Many growth factors are involved in these processes.[2-9] Vascular endothelial growth factor (VEGF) plays an important role in the development of EC and tube formation. Platelet-derived growth factor (PDGF)-BB produced from EC induces recruitment of MC to the proximity of EC forming the tube.[10] Subsequently, MC adhere to EC for the formation of a structurally stable blood vessel. It has been reported that this cell adhesion between EC and MC occurs when angiopoietin-1 (Ang1), produced from MC, stimulates Tie2, a receptor tyrosine kinase on EC.[11-13] Therefore, Ang1 is involved in the maturation process of blood vessels.

So far four types of Tie2 ligands (Ang1 to Ang4) have been isolated.[14] Ang1 binds to Tie2 and activates it by inducing dimerization of Tie2, which results in phosphorylation of the kinase domain of Tie2. Ang2 also binds to Tie2; however, Ang2 does not induce phosphorylation of Tie2 at physiological concentration. Therefore, Ang2 has been suggested to work as a naturally occurring antagonist of Ang1. Tie2 activation by Ang1 induces cell adhesion to the extracellular matrix via integrin activation,[15] and disruption of the interaction between EC and MC by targeted mutation of Tie2[11,12] or overexpression of Ang2 in EC inhibits

angiogenesis.[16] Ang2 expression is induced in EC under conditions of tissue hypoxia. However, Ang1 expression is not altered by hypoxia and it is expressed constitutively in MC. Therefore, it has been suggested that Ang1 induces cell adhesion between EC and MC, resulting in the stabilization of blood vessel structure and silencing of angiogenesis. In contrast, Ang2 induces sprouting angiogenesis by the inhibition of cell adhesion between EC and MC.

It is widely accepted that high-level Ang2 expression in tumors both induces hypervascularity by promoting sprouting angiogenesis and enhances tumor growth; this was confirmed in clinical samples of tumors and studies of Ang2 overexpression in tumor xenograft models.[17] However, the role of Ang1 in tumor angiogenesis is less clear. In a xenograft model using Hela cells, knockdown of the *Ang1* gene led to decreased tumor growth and angiogenesis[18] and overexpression of Ang1 promoted angiogenesis, resulting in enhanced tumor growth.[19] Therefore, in this case, Ang1 seems to stimulate angiogenesis. In contrast, overexpression of Ang1 in breast[20] and colon cancer cells[21] results in decreased tumor growth and angiogenesis. We hypothesized that these controversial results may have arisen from differences relating to whether MC occur in proximity to blood vessels or not. Ang1 induces cell-to-cell adhesion between MC and EC for the structural stabilization of blood vessels and also induces spreading of EC.[22,23] In the former function sprouting angiogenesis must be restricted, and in the latter function sprouting angiogenesis is induced. To test whether Ang1 has the ability to alter tumor growth affected by the abundance of MC in the tumor environment, in the present study we examined blood vessel formation in two different types of xenograft tumor model: the colon cancer cell line HT29 and the prostate cancer cell line PC3.

Materials and Methods

Mice, cell lines, and tumors. The HT29 (human colon cancer) and PC3 (human prostate cancer) cell lines were cultured in RPMI-1640 (Sigma, St Louis, MO, USA) supplemented with 10% fetal bovine serum (Sigma), 100 U/mL penicillin, 100 µg/mL streptomycin, and 4 µg/mL L-glutamine (only for HT29 cells) at 37 °C in 5% CO_2, 95% air. Colon26 (mouse colon cancer), B16 (mouse melanoma), and LLC (mouse lung cancer) cell lines were cultured in Dulbecco's modified Eagle's medium (Sigma) supplemented with 10% fetal bovine serum, 100 U/mL penicillin, and 100 µg/mL streptomycin at 37 °C in an atmosphere of 5% CO_2, 95% air.

The mouse Ang1 (mAng1) expression plasmid was constructed by replacing the coding region of enhanced green fluorescent protein (EGFP) in the pEGFP-N1 vector (Clonetech, Palo Alto, CA, USA) with the mAng1-FLAG gene. It was transfected into each cell line using Lipofectamine 2000 reagent (Invitrogen, Carlsbad, CA, USA). After transfection, the cells were cultured in medium supplemented with G418 (Gibco, Rockville, MD, USA;

[1]To whom correspondence should be addressed. E-mail: ntakaku@biken.osaka-u.ac.jp

1000 μg/mL for HT29 cells; 800 μg/mL for PC3 cells) to obtain cells stably expressing mAng1 (HT29–Ang1 and PC3–Ang1). Mock vector was used for obtaining control cells (HT29–mock and PC3–mock). The mAng1 gene was transduced into colon26, B16, and LLC cells as described above and cells stably expressing mAng1 were selected with G418 (800 μg/mL). Expression of the *mAng1* gene was confirmed by real-time polymerase chain reaction (PCR) and reverse transcription (RT)–PCR.

KSN female nude mice (7–8 weeks of age), C57BL/6 female mice (7–8 weeks of age), and BALB/c female mice (7–8 weeks of age) were purchased from Japan SLC (Shizuoka, Japan). Subcutaneous xenografts were established by injecting 3.6×10^6 cells into the flanks of mice. Tumor dimensions were measured using a caliper and volume was calculated according to the formula $V = (\text{short side})^2 \times (\text{long side})/2$. The mice were killed using ethyl ether anesthesia. Immediately after removal, tumors were fixed for 2 h at 4 °C in 4% paraformaldehyde–phosphate-buffered saline (pH 7.5) (PBS) and washed with PBS. Subsequently, samples were soaked in 20% sucrose–PBS until sinking. Then, samples were frozen in optimal cutting temperature (OCT) compound (Sakura Finetechnical, Tokyo, Japan) in preparation for subsequent immunohistochemical analyses.

Reverse transcription–polymerase chain reaction and quantitative real-time polymerase chain reaction. Total RNA was isolated from cultured cells with ISOGEN (Nippon Gene, Tokyo, Japan) following the manufacturer's instructions and 1 μg of the RNA was reverse transcribed using Advantage RT supplied with the PCR kit (Clonetech) using the manufacturer's instruction.

cDNA was quantified by real-time PCR on a Mx3000P (Stratagene, La Jolla, CA, USA). Real-time PCR was carried out using Platinum SYBR Green qPCR SuperMix-UDG (Invitrogen) according to manufacturer's instructions. The amplification step consisted of 40 cycles at 95°C for 15 s and 60°C for 30 s. The relative mRNA expression level was calculated by the comparative threshold cycle (Ct) method, and mouse glyceraldehyde-3-phosphate dehydrogenase (mGAPDH) was used as an internal normalization control. Specific oligonucleotide primers were as follows: mAng1, sense 5′-CTC GTC AGA CAT TCA TCA TCC AG-3′ and antisense 5′-CAC CTT CTT TAG TGC AAA GGC T-3′; for mGAPDH, sense 5′-AGG TCG GTG TGA ACG GAT TTG-3′ and antisense 5′-TGT AGA CCA TCT AGT TGA GGT CA-3′.

Immunohistological analysis. Tissue fixation and immunohistological analyses of tissue sections were carried out as described previously.[23,24] Briefly, the fixed specimens were embedded in OCT compound and sectioned at 20 μm. For the immunofluorescence analyses for counting the number of MC, Cy3-conjugated mouse anti-α-smooth muscle actin (SMA) monoclonal antibody (Sigma) was used for staining MC and nuclei were counterstained with TOPRO3 (Invitrogen). Nuclei of α-SMA-stained cells were counted (at ×400 magnification) in five different fields (0.0531 mm²) of the core and peripheral regions in each tumor.

For the immunohistochemical analyses of tumor vessel density, rat antimouse CD31 antibody (BD Biosciences, San Diego, CA, USA) and horseradish peroxidase (HRP)-conjugated mouse anti-human α-SMA antibody (Dako, Carpinteria, CA, USA) were used for primary antibodies. As a secondary antibody for anti-CD31, alkaline phosphatase (AP)-conjugated goat antirat Ig (BioSource, Camarillo, CA, USA) was used. For the visualization of AP and HRP, a 5-bromo-4-chloro-3-indoxyl phosphate and nitro blue tetrazolium chloride (BCIP/NBT) substrate system (Dako) and diaminobenzidine (Dojindo, Kumamoto, Japan) were used, respectively. CD31-stained vessels were counted (at ×50 magnification) in a 5.73-mm² field of the core and peripheral regions of three different tumors.

For the immunofluorescence analyses of tumor vessels covered with MC, rat antimouse CD31 monoclonal antibody and Cy3-conjugated antihuman α-SMA antibody were used as primary antibodies. For anti-CD31 antibody, Alexa488-conjugated antirat

was used as a secondary antibody (Invitrogen). Nuclear staining was carried out using TOPRO3. The degree to which MC adhered to and covered the EC in the blood vessels was evaluated in five fields (0.0531 mm²) at the core and peripheral regions of three different tumors. Blood vessels were divided into three groups according to the degree that MC covered the EC (0–33%, 33–67%, and 67–100%). The average percentage of counted vessels at each degree relative to the total counted vessels was calculated for each tumor.

For all experiments, pictures of fluorescence-stained sections were taken by confocal microscopy (LSM510; Carl Zeiss Micro-Imaging, Oberkochen, Germany). Pictures of immunohistochemical-stained sections were taken by digital microscopy (DM5500B; Leica Microsystems, Nussloch, Germany). Images were processed using Adobe Photoshop 7.0 software (Adobe Systems, San Jose, CA, USA).

Analyses of tumor vessel permeability. Tumor vessel permeability was analyzed by detecting leakage of an injected antibody. Rat anti-B220 antibody (250 μg) was injected into the tail vein of the subcutaneous xenograft model mouse (on day 14 after inoculation of PC3 or PC3–Ang1 cells, or on day 28 after inoculation of HT29 or HT29–Ang1 cells). One hour after injection, tumors were removed and sections were prepared. For detection of leaked B220 antibody, HRP-conjugated antirat IgG (BioSource; diluted 1:1000) was used.

Statistical analysis. Results are expressed as the mean ± SD. Student's *t*-test was used for statistical analysis. Differences were considered statistically significant if the *P*-value was less than 0.05.

Results

Localization of mural cells in the xenograft model using colon cancer and prostate cancer cell lines. It is widely accepted that lack of MC adhesion to EC induces endothelial hyperplasia, resulting in abnormal vascular morphogenesis and leakiness, especially in the core region of tumors.[25] In a xenograft model using the human prostate cancer cell line PC3, we confirmed that there are fewer MC in the core region (center) of a tumor compared with the peripheral region (edge) (Fig. 1Aa,b,B). In contrast, when the human colon cancer cell line HT29 was used for this xenograft model, we found that MC were equally distributed in the core and peripheral regions of the tumor (Fig. 1Ac,d,B). Moreover, the number of MC in the tumors formed by HT29 cells was higher than that in tumors formed by PC3 cells. As reported previously, ectopic overexpression of Ang1 in HT29 cells results in decreased tumor growth.[21] Based on that previous report and our present finding, it may be inferred that the abundance of MC localizing to the tumor alters tumor growth, affecting blood vessel formation by Ang1. Therefore, to test this possibility, we tried to induce mAng1 in both PC3 and HT29 tumor cells (Fig. 2a; PC3–Ang1 and HT29–Ang1) and to observe the proliferation of MC in a tumor xenograft model (Figs 1B,2b). Our results indicated that Ang1 did not affect the number of MC in either tumor by PC3 or HT29 cells.

Angiopoietin-1 alters tumor growth. To examine the effect of Ang1 on tumor growth, we investigated whether PC3 and HT29 cells express human Ang1 endogenously. However, we could not detect human Ang1 in PC3 or HT29 cells cultured *in vitro*. It is possible that tumor cells inoculated into mice express human Ang1 by receiving stimuli present in their environment, but we could not detect human Ang1 in the peripheral or core regions of PC3 and HT29 tumors (data not shown).

Transfection of HT29 cells with Ang1 expression vector significantly reduced the growth of tumors derived from HT29–Ang1 cells compared with HT29 parental cells or HT29 cells transduced with mock vector (HT29–mock) (Fig. 3a), confirming a previous report.[21] In contrast, when Ang1 was expressed in PC3 cells by transfection with Ang1 expression vector, the growth of tumors
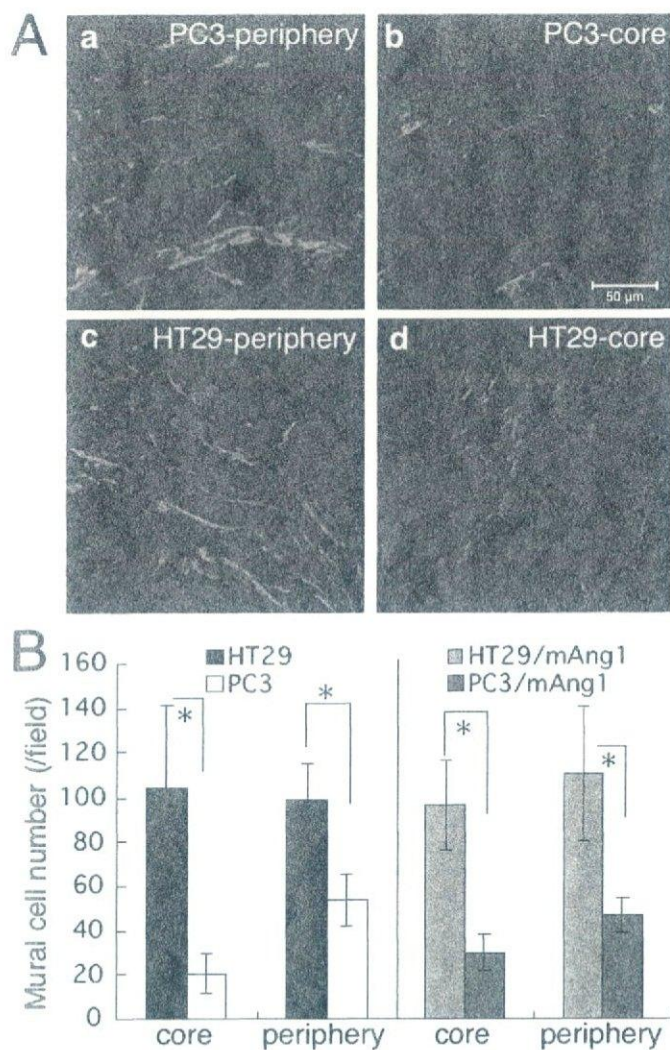
Fig. 1. Localization of mural cells in the tumor environment. (A) Tissue sections from (a,b) PC3 and (c,d) HT29 tumors from the (a,c) peripheral and (b,d) core regions were stained with anti-α-smooth muscle actin antibody (red). Nuclei were counterstained with TOPRO3 (blue). Scale bar = 50 μm. (B) Statistical evaluations of the number of mural cells in the core and peripheral regions of individual tumors are indicated. Data show the means ± SD from five random fields. *$P < 0.01$. mAng1, mouse angiopoietin-1.

Fig. 2. Effect of the overexpression of angiopoietin-1 (Ang1) in tumor cells on the prevalence of mural cells in tumors. (A) Relative expression of mouse Ang1 (mAng1) mRNA in PC3 and HT29 cells, PC3 and HT29 cells transfected with mock vector (PC3–mock and HT29–mock, respectively), and PC3 and HT29 cells transfected with a vector containing the mouse Ang1 gene (PC3–Ang1 and HT29–Ang1, respectively) detected by real-time polymerase chain reaction analysis (upper) and further confirmed by reverse transcription–polymerase chain reaction analysis (lower). Glyceraldehyde-3-phosphate dehydrogenase (GAPDH) was used as an internal control. (B) Tissue sections from (a,b) PC3–Ang1 and (c,d) HT29–Ang1 tumors from the (a,c) peripheral and (b,d) core regions were stained with anti-α-smooth muscle actin antibody (red). Nuclei were counterstained with TOPRO3 (blue). Scale bar = 50 μm.

derived from the cells was enhanced significantly compared to that of PC3 parental cells or PC3 cells transduced with mock vector (PC3–mock). We evaluated tumor growth using several Ang1-induced subclones derived from HT29 and PC3 cells and obtained similar results (Fig. 3).

Angiopoietin-1 enhances angiogenesis in the core region of PC3 tumors. As noted, Ang1 expression in the tumor enhanced tumor growth derived from PC3 cells but inhibited the growth of tumors derived from HT29 cells. We therefore hypothesized that Ang1 enhanced tumor angiogenesis in PC3 tumors but suppressed it in HT29 tumors. As such, we evaluated the number of blood vessels in tumors derived from PC3, PC3–Ang1, HT29, and HT29–Ang1 cells. The number of blood vessels in the peripheral region of tumors was comparable between tumors derived from PC3 and PC3–Ang1 (data not shown). As expected, blood vessel formation was enhanced in tumors from PC3–Ang1 cells in the core region of tumors (Fig. 4Aa,b,B). However, an unexpected finding was that the number of blood vessels in tumors derived from HT29
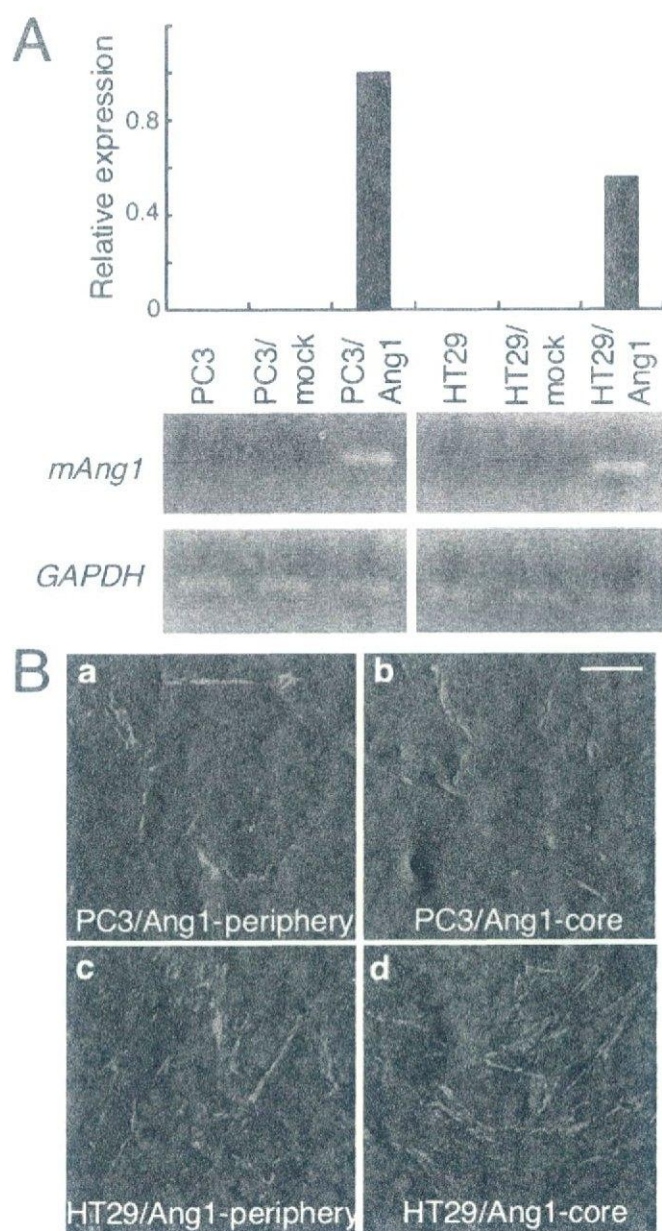
and HT29–Ang1 cells was not different in the core (Fig. 4Ac,d,B) and peripheral regions of tumors (data not shown). The numbers of blood vessels in PC3 tumors compared with PC3–mock tumors, and in HT29 tumors compared with HT29–mock tumors were not greatly different. Therefore, Ang1-mediated suppression of tumor growth was not induced by the inhibition of tumor angiogenesis in HT29 cells.
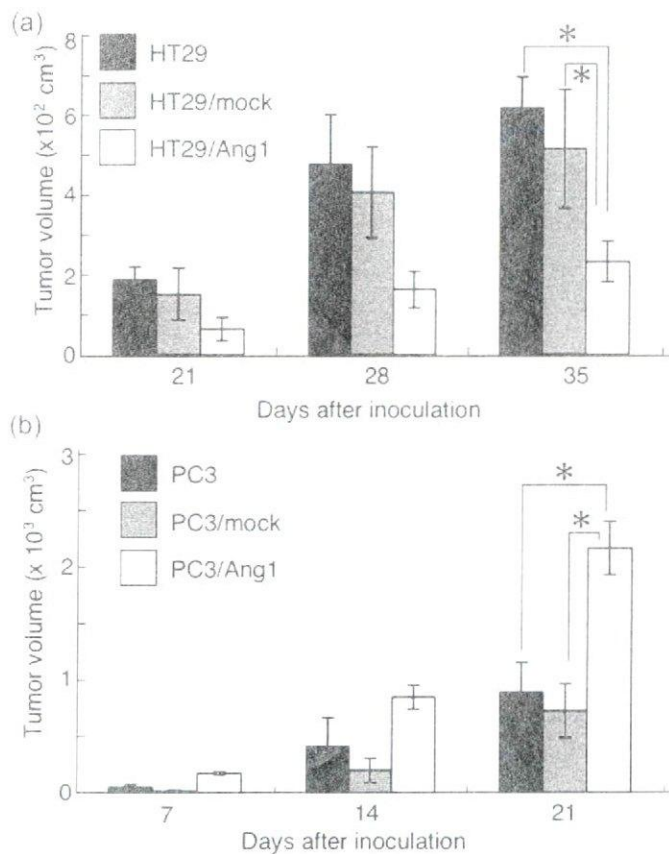
Satoh *et al.*

Fig. 3. Effect of angiopoietin-1 (Ang1) overexpression in tumor cells on tumor growth. (a) Tumor growth was evaluated by measuring tumor volume on days 21, 28, and 35 after inoculation of tumor cells as indicated. $*P < 0.03$ ($n = 3$). (b) Tumor growth was evaluated by measuring tumor volume on days 7, 14, and 21 after inoculation of tumor cells as indicated. $*P < 0.03$ ($n = 3$).

Fig. 4. Effect of angiopoietin-1 (Ang1) overexpression in tumor cells on the number of blood vessels. (A) Tissue sections from the core region of tumors derived from (a) PC3, (b) PC3–Ang1, (c) HT29, and (d) HT29–Ang1 were stained with anti-α-smooth muscle actin antibody (brown) and anti-CD31 antibody (dark blue). Tumors were dissected from mice on day 14 after the inoculation of tumor cells into mice in the case of PC3 and PC3–Ang1 tumors, and on day 28 after inoculation in the case of HT29 and HT29–Ang1 tumors. Scale bar = 500 µm. (B) Statistical evaluations of the number of blood vessels in the core region of individual tumors are indicated. Data show means ± SD from three different tumors. $*P < 0.03$ ($n = 3$).

Angiopoietin-1-induced mural cell adhesion to endothelial cells in tumor vessels. Finally, we determined the effect of Ang1 on MC adhesion to EC in tumors. For this purpose, we divided blood vessels into three groups according to the percentage of MC that adhered to and covered the EC (0–33%, poorly matured; 33–67%, moderately matured; and 67–100%, highly matured) and evaluated the maturation of blood vessels in tumors. In the case of PC3 tumors, half of the blood vessels were highly matured in the peripheral region of tumors (Fig. 5Aa,e) and Ang1 overexpression slightly enhanced blood vessel maturation (Fig. 5Ac,e). However, in the core region of PC3 tumors, most blood vessels were poorly matured (Fig. 5Ab,f). Ang1 overexpression induced blood vessel maturation in the core region of PC3–Ang1 tumors; however, compared to the peripheral region, most of the blood vessels were in the poorly and moderately matured part (Fig. 5Ad,f). In case of HT29 tumors, most blood vessels in the peripheral region of the tumors were highly matured (Fig. 5Ba,e) and Ang1 overexpression in HT29 cells enhanced blood vessel maturation in the peripheral region of the tumors (Fig. 5Bc,e). Compared to PC3 tumors, half of the blood vessels in the core region of HT29 tumors were highly matured originally (Fig. 5Bb,f) and Ang1 in HT29 cells enhanced maturation of the blood vessels (Fig. 5Bd,f). Therefore, a large difference was observed between PC3 tumors and HT29 tumors in the extent of adhesion of MC to EC in the core region of tumors; that is, lack of MC adhesion to EC was broadly observed in the core region of PC3 tumors, which is a well-known characteristic of most of tumors. On the other hand, in the case of HT29 tumors, blood vessels were well matured in
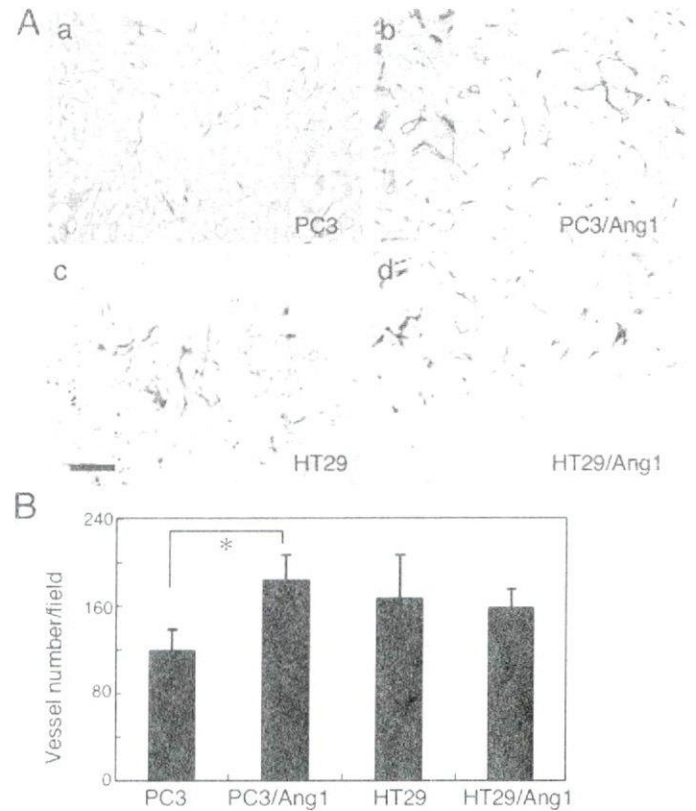
the core region as well as the peripheral region of the tumors. The maturation of blood vessels in PC3 compared with PC3–mock tumors, and in HT29 compared with HT29–mock tumors was not notably different. Therefore, we concluded that the mechanism whereby Ang1 alters tumor growth depends on the proportion of mature blood vessels in the tumors.

Discussion

In the present study, we evaluated the function of Ang1 for tumor growth and found that Ang1 alters tumor growth depending on whether blood vessels in tumors are mature or not. Ang1 has paradoxical roles in angiogenesis: Tie2 activation on EC by Ang1 induces cell adhesion between EC and MC,[11,12,15] resulting in the silencing of angiogenesis, and Tie2 activation induces spreading of EC[22,23] in the absence of MC adhesion to EC, resulting in the promotion of angiogenesis. In the case of PC3 tumors, there was a notable lack of MC adhesion in the core region of tumors. Although Ang1 overexpression induced a small degree of maturation of blood vessels in this region, most of the blood vessels were immature. Therefore, Ang1 induced sprouting of EC, resulting in enhanced angiogenesis and tumor growth (type A in Fig. 6). However, in the case of HT29 tumors, blood vessels were well matured in both the peripheral and core regions of the tumors and MC not adhering to EC were also observed
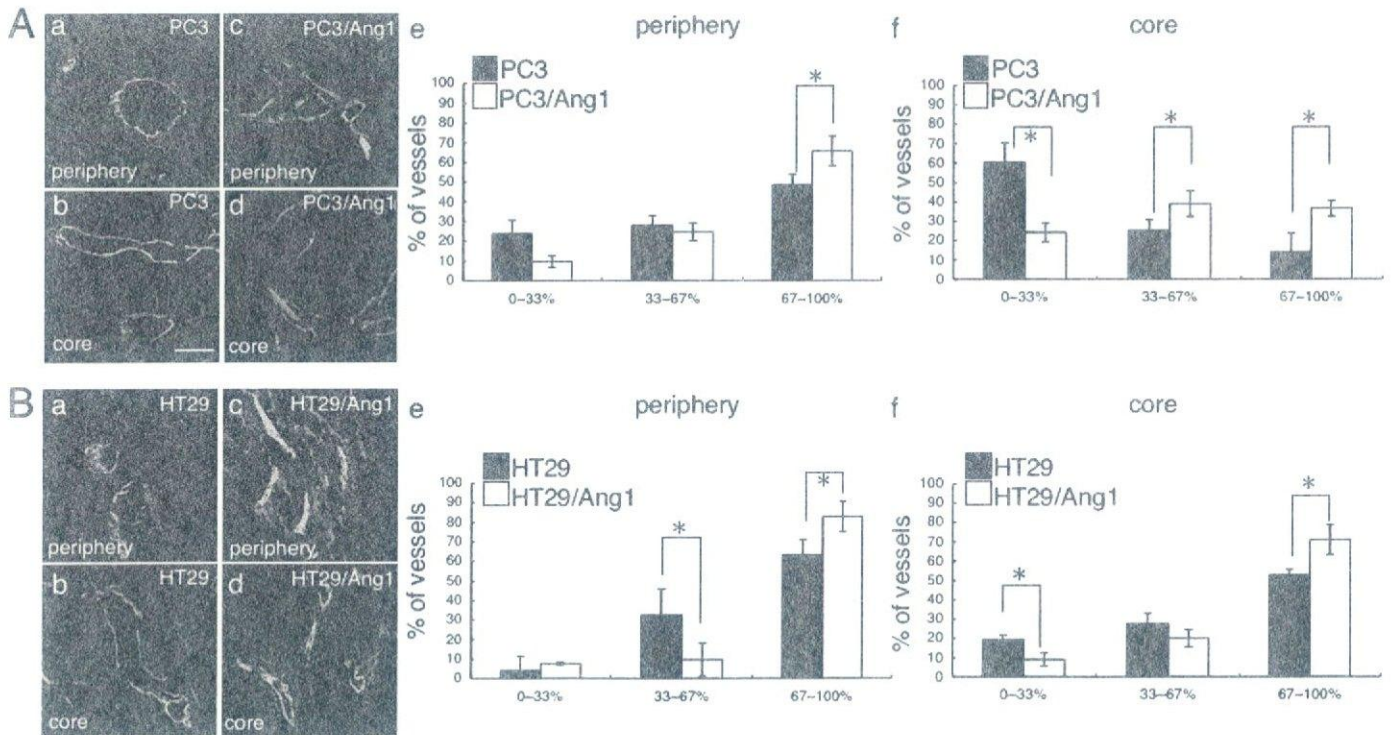
Fig. 5. Effect of angiopoietin-1 (Ang1) overexpression in tumor cells on the maturation of blood vessels. (A) Tissue sections from (a,b) PC3 and (c,d) PC3–Ang1 tumors from the (a,c) peripheral and (b,d) core regions were stained with anti-α-smooth muscle actin (SMA) antibody (red) and anti-CD31 antibody (green). Nuclei were counterstained with TOPRO3 (blue). Tumors were dissected from mice on day 14 after inoculation of tumor cells into mice in the case of PC3 and PC3–Ang1 tumors, and on day 28 in the case of HT29 and HT29–Ang1 tumors. Scale bar = 50 μm. (e,f) Statistical evaluations of the maturation of blood vessels from the (e) peripheral and (f) core regions of tumors. Data show means ± SD from five random fields. *$P < 0.03$ ($n = 5$). (B) Tissue sections from (a,b) HT29 and (c,d) HT29–Ang1 tumors from the (a,c) peripheral and (b,d) core regions were stained with anti-α-SMA (red) and anti-CD31 (green) antibodies. Nuclei were counterstained with TOPRO3 (blue). (e,f) Statistical evaluations of the maturation of blood vessels in the (e) peripheral and (f) core regions of tumors. Data show means ± SD from five random fields. *$P < 0.03$ ($n = 5$).

Table 1. Effect of angiopoietin-1 (Ang1) on tumor growth in association with mural cell (MC) incidence

| Tumor | MC incidence | | Effect of Ang1 on tumor growth | Ang1 expression fold increase[†] |
	Periphery	Core		
Human				
PC3	Observed frequently	Not observed frequently	Enhanced	
HT29	Observed frequently	Observed frequently	Suppressed	
Mouse				
Colon26 (colon cancer)	Observed frequently	Not observed frequently	Enhanced	114.5
B16 (melanoma)	Observed frequently	Observed frequently	Suppressed	110.7
LLC (lung cancer)	Observed frequently	Observed frequently	Suppressed	92.4

†Fold increase of mouse Ang1 mRNA expression in tumor cells transfected with Ang1 expression vector compared with Ang-1 expression vector non-induced tumor cells. Data are representative of three independent real-time polymerase chain reaction analyses.

near the blood vessels (Fig. 5Bb). In this situation, overexpression of Ang1 enhanced the formation of highly mature blood vessels (type B in Fig. 6). As seen with human tumor cell lines, when mouse tumor cell lines were used for the tumor xenograft model, Ang1 altered tumor growth depending on the incidence of MC in the core region of the tumor (Table 1).

In theory, MC adhesion to EC may inhibit angiogenesis; however, our results indicated that enhancement of blood vessel maturation by Ang1 did not alter the number of blood vessels in HT29–Ang1 tumors compared with HT29 tumors. The reason why enhancement of blood vessel maturation inhibited tumor growth without suppression of angiogenesis is not clear in the present study. A previous report showed that transduction of Ang1 into colon carcinoma cells resulted in the suppression of tumor growth with the inhibition of angiogenesis.[21] However, another report showed that Ang1 inhibits squamous cell carcinoma growth, not by affecting vascular density but by enhancing blood vessel maturation.[26] Our result is comparable to that of the latter report. How blood vessel maturation inhibits tumor growth is not clearly understood at present and further analysis is required. However, a functional change in permeability from blood vessels for the penetration of oxygen and nutrients into deep sites of tumors[27] may be critical for regulating tumor growth by Ang1. Indeed, when permeability was compared in tumors, Ang1 inhibited permeability in the core region of HT29 tumors and, conversely, Ang1 enhanced permeability in the core region of PC3 tumors (Fig. 7). However, Ang1 did not affect permeability in the peripheral region of tumors in either HT29 or PC3 tumors (data not
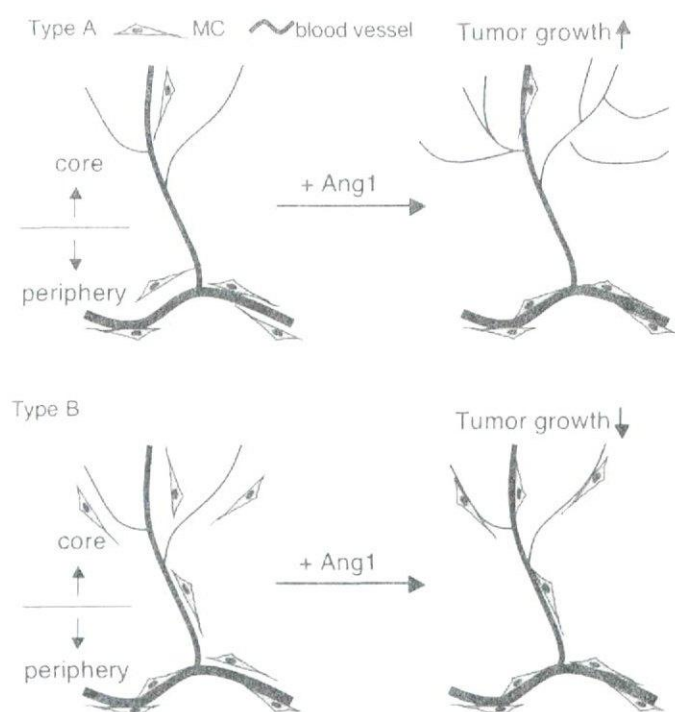
Fig. 6. Summary of angiopoietin-1 (Ang1) function in two types of tumors. In a type A tumor, for example PC3, the incidence of mural cells (MC) is very low and blood vessels are not highly mature, especially in the core region of the tumor. In this type of tumor, Ang1 induced sprouting angiogenesis rather than maturation of blood vessels, resulting in enhancement of tumor growth. On the other hand, in a type B tumor, for example HT29, the blood vessels are highly mature in both the core and peripheral regions. In this type of tumor, Ang1 enhanced maturation of blood vessels rather than sprouting angiogenesis. In this case, suppression of permeability may be one of the reasons for the inhibition of tumor growth.
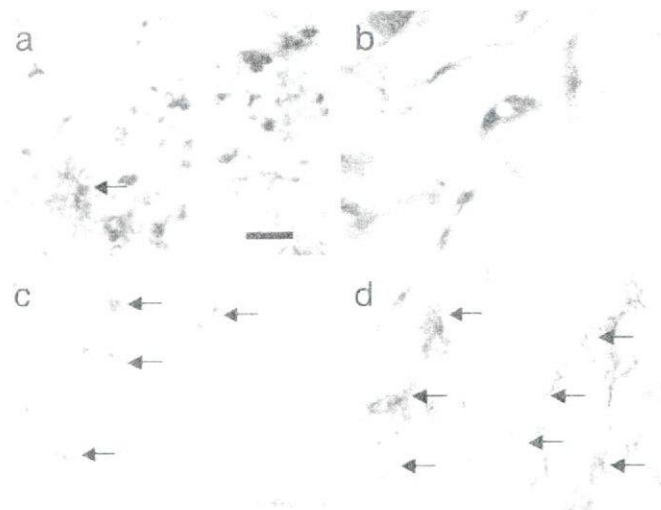

Fig. 7. Alteration of vascular permeability by angiopoietin-1 (Ang1) in tumors. Extravasation of anti-B220 antibody from blood vessels is demonstrated by staining with horseradish peroxidase-conjugated antirat IgG in the core regions of (a) HT29, (b) HT29–Ang1, (c) PC3, and (d) PC3–Ang1 tumors (brown color indicated by arrows). Scale bar = 50 μm.

shown). These findings suggested that maturation of blood vessels in the core region brought about by Ang1 resulted in the suppression of tumor growth in the case of HT29 tumors and that induction of abundant immature blood vessel formation in the core region by Ang1 resulted in enhancement of tumor growth in the case of PC3 tumors.

It is widely accepted that an imbalance of proangiogenic and antiangiogenic factors, especially a dominance of proangiogenic factors, in the tumor environment induces abnormal blood vessel formation.[28] This abnormality in blood vessels includes leakiness, tortuousness, and dilation, which are caused mainly by loss of MC adhesion to EC.[25] These abnormalities contribute to the heterogeneity of tumor blood flow, resulting in hypoxia with interstitial hypertension.[25] Hypoxia induces angiogenesis, which leads to continuing proliferation of tumor cells. Therefore, antitumor therapies targeting angiogenesis have been developed to destroy the tumor vasculature. However, recently, new concepts have emerged that are based on normalization of abnormal blood vessels in the tumor environment by inducing MC adhesion to EC to more effectively deliver oxygen and drugs.[29] This idea came from evidence that administration of a single antiangiogenic inhibitor is not effective for cancer therapy[30] but a combination

of antiangiogenic inhibitors as anticancer therapy is more effective for the survival rate of colorectal cancer patients.[31] However, as observed in our study, maturation of blood vessels by adhesion of MC to EC was sufficient to inhibit HT29 tumor growth without another anticancer drug. Therefore, downregulation of proangiogenic factors such as VEGF, Ang2, or upregulation of antiangiogenic factors such as Ang1 and PDGF-BB may exert normalization or maturation of blood vessels by different mechanisms.

In the present study, however, Ang1 induced angiogenesis as well as the maturation of blood vessels in PC3 tumors, resulting in the enhancement of tumor growth. From this result, it is apparent that Ang1 administration is effective for tumor suppression when MC are observed abundantly in the entire tumor environment. For the clinical application of Ang1 or Tie2 agonist in tumors, pathological diagnosis before treatment is required. Moreover, recruitment of MC into the tumor environment may be a way to augment the action of Tie2 agonist in tumors. Compared to PC3 tumors, more MC were observed in HT29 tumors. We tried to distinguish this difference by the expression of PDGF-BB, which induces recruitment of MC.[10] However, PDGF-BB expression was not different between HT29 and PC3 cells. Therefore, further information on the molecular mechanism by which MC recruitment is induced abundantly in HT29 tumors compared with PC3 tumors would shed light on the maturation process of blood vessels in the tumor environment.

Acknowledgments

References

1 Risau W. Mechanisms of angiogenesis. *Nature* 1997; **386**: 671–4.
2 Gale NW, Yancopoulos GD. Growth factors acting via endothelial cell-specific receptor tyrosine kinases: VEGFs, angiopoietins, and ephrins in vascular development. *Genes Dev* 1999; **13**: 1055–66.
3 Oettgen P. Transcriptional regulation of vascular development. *Circ Res* 2001; **89**: 380–8.
4 Carmeliet P. Angiogenesis in health and disease. *Nat Med* 2003; **9**: 653–60.
5 Gerhardt H, Betsholtz C. Endothelial–pericyte interactions in angiogenesis. *Cell Tissue Res* 2003; **314**: 15–23.

6 Simon MC. Vascular morphogenesis and the formation of vascular networks. *Dev Cell* 2004; **6**: 479–82.

7 Wang HU, Chen ZF, Anderson DJ. Molecular distinction and angiogenic interaction between embryonic arteries and veins revealed by ephrin-B2 and its receptor Eph-B4. *Cell* 1998; **93**: 741–53.

8 Adams RH, Wilkinson GA, Weiss C *et al.* Roles of ephrinB ligands and EphB receptors in cardiovascular development: demarcation of arterial/venous domains, vascular morphogenesis, and sprouting angiogenesis. *Genes Dev* 1999; **13**: 295–306.

9 Zhong TP, Childs S, Leu JP, Fishman MC. Gridlock signalling pathway fashions the first embryonic artery. *Nature* 2001; **414**: 216–20.

10 Lindahl P, Johansson BR, Leveen P, Betsholtz C. Pericyte loss and micro-aneurysm formation in PDGF-B-deficient mice. *Science* 1997; **277**: 242–5.

11 Dumont DJ, Gradwohl G, Fong GH *et al.* Dominant-negative and targeted null mutations in the endothelial receptor tyrosine kinase, tek, reveal a critical role in vasculogenesis of the embryo. *Genes Dev* 1994; **8**: 1897–909.

12 Sato TN, Tozawa Y, Deutsch U *et al.* Distinct roles of the receptor tyrosine kinases Tie-1 and Tie-2 in blood vessel formation. *Nature* 1995; **376**: 70–4.

13 Suri C, Jones PF, Patan S *et al.* Requisite role of angiopoietin-1, a ligand for the Tie-2 receptor, during embryonic angiogenesis. *Cell* 1996; **87**: 1171–80.

14 Valenzuela DM, Griffiths JA, Rojas J *et al.* Angiopoietins 3 and 4: diverging gene counterparts in mice and humans. *Proc Natl Acad Sci USA* 1999; **96**: 1904–9.

15 Takakura N, Huang XL, Naruse T *et al.* Critical role of the TIE2 endothelial cell receptor in the development of definitive hematopoiesis. *Immunity* 1998; **9**: 677–86.

16 Maisonpierre PC, Suri C, Jones PF *et al.* Angiopoietin-2, a natural antagonist for Tie2 that disrupts *in vivo* angiogenesis. *Science* 1997; **277**: 55–60.

17 Metheny-Barlow LJ, Li LY. The enigmatic role of angiopoietin-1 in tumor angiogenesis. *Cell Res* 2003; **13**: 309–17.

18 Shim WS, Teh M, Mack PO, Ge R. Inhibition of angiopoietin-1 expression in tumor cells by an antisense RNA approach inhibited xenograft tumor growth in immunodeficient mice. *Int J Cancer* 2001; **94**: 6–15.

19 Shim WS, Teh M, Bapna A *et al.* Angiopoietin 1 promotes tumor angiogenesis and tumor vessel plasticity of human cervical cancer in mice. *Exp Cell Res* 2002; **279**: 99–309.

20 Hayes AJ, Huang WQ, Yu J *et al.* Expression and function of angiopoietin-1 in breast cancer. *Br J Cancer* 2000; **83**: 1154–60.

21 Ahmad SA, Liu W, Jung YD *et al.* The effects of angiopoietin-1 and -2 on tumor growth and angiogenesis in human colon cancer. *Cancer Res* 2001; **61**: 1255–9.

22 Witzenbichler B, Maisonpierre PC, Jones P, Yancopoulos GD, Isner JM. Chemo-tactic properties of angiopoietin-1 and -2, ligands for the endothelial-specific receptor tyrosine kinase Tie2. *J Biol Chem* 1998; **273**: 18 514–21.

23 Takakura N, Watanabe T, Suenobu S *et al.* A role for hematopoietic stem cells in promoting angiogenesis. *Cell* 2000; **102**: 199–209.

24 Yamada Y, Takakura N. Physiological pathway of differentiation of hemato-poietic stem cell population into mural cells. *J Exp Med* 2006; **203**: 1055–65.

25 Hellström M, Gerhardt H, Kalén M *et al.* Lack of pericytes leads to endothelial hyperplasia and abnormal vascular morphogenesis. *J Cell Biol* 2001; **153**: 543–53.

26 Hawighorst T, Skobe M, Streit M *et al.* Activation of the tie2 receptor by angiopoietin-1 enhances tumor vessel maturation and impairs squamous cell carcinoma growth. *Am J Pathol* 2002; **160**: 1381–92.

27 Hamzah J, Jugold M, Kiessling F *et al.* Vascular normalization in Rgs5-deficient tumours promotes immune destruction. *Nature* 2008; **453**: 410–14.

28 Jain RK. Molecular regulation of vessel maturation. *Nat Med* 2003; **9**: 685–93.

29 Jain RK. Normalization of tumor vasculature: an emerging concept in antiangiogenic therapy. *Science* 2005; **307**: 58–62.

30 Yang JC, Haworth L, Sherry RM *et al.* A randomized trial of bevacizumab, an anti-vascular endothelial growth factor antibody, for metastatic renal cancer. *N Engl J Med* 2003; **349**: 427–34.

31 Hurwitz H, Fehrenbacher L, Novotny W *et al.* Bevacizumab plus irinotecan, fluorouracil, and leucovorin for metastatic colorectal cancer. *N Engl J Med* 2004; **350**: 2335–42.

Involvement of MDR1 Function in Proliferation of Tumour Cells

Shin-Ya Katoh, Masaya Ueno and Nobuyuki Takakura*

Department of Signal Transduction, Research Institute for Microbial Diseases, Osaka University, 3-1 Yamada-oka, Suita, Osaka 565-0871, Japan

Mdr1 is a multi-drug-resistance protein, a member of the adenosine triphosphate-binding cassette family of drug transporters. Mdr1 is expressed in wide variety of cells and limits absorption of toxicants into the body or tissue; however, it is also expressed in many cancer cells and can render tumour cells resistant to many anti-cancer drugs. Mdr1 is well studied as a multi-drug resistance transporter, but little is known regarding its other role in tumour cells. In the present study, we investigated *mdr1* function in tumour cell proliferation. We silenced the *mdr1* gene in tumour cells by using an RNA interference method that employed short hairpin RNA. The result showed that knockdown of *mdr1* gene suppressed tumour cell proliferation *in vitro*, and induced the passage of the cell cycle into the G1/G0 phase. Furthermore, in a mice xenograft tumour formation assay, *mdr1* knockdown of tumour cells inhibited tumour expansion. These results suggest that Mdr1 plays a role in regulation of tumour cells proliferation.

Key words: Mdr1, tumour, proliferation, RNAi, drug resistance.

Abbreviations: ABC transporter, ATP-binding cassette transporter; CyA, cyclosporine A; DXR, doxorubicin; BrdU, bromodeoxyuridine; ERK1/2, extracellular signal-regulated kinase ½; GAPDH, glyceraldehyde 3-phosphate dehydrogenase; MDR, multi-drug resistance; MEFs, mouse embryonic fibroblasts; Mrp, multi-drug resistance associated protein; MTT, 3-[4,5-dimethylthiazol-2-yl]- 2,5-diphenyl-tetrazolium bromide; PI, propidium iodide; RNAi, RNA interference; Rs, reserpine; RT-PCR, reverse transcription-polymerase chain reaction; shRNA, short hairpin RNA.

The expression of multi-drug resistance (MDR) in tumour cells remains one of the most significant causes of failure in anti-tumour chemotherapy (1). It has been widely accepted that the mechanisms leading to chemoresistance of tumour cells is the increased activity of transporter proteins (2). MDR1/P-glycoprotein (p-gp) is a well-characterized transporter protein and various types of compounds and techniques for its inhibition have been developed (3–5). For this purpose, knowledge of the physiological function of MDR1 should provide a means for the suppression of MDR1 without side effects.

MDR1 belongs to a superfamily of ATP-binding cassette (ABC) transporters and is widely expressed in tissues and cells, including the blood–brain barrier, proximal tubular renal epithelium, gut, liver, adrenal glands, lymphocytes, haematopoietic stem cells and cancer stem cells (6–8). The physiological role of MDR1 is in cellular detoxification of bacterial products, hormone secretion and transport of some metabolites (9–11). This phenomenon is due to the ability of MDR1 to pump several types of molecules from the inside of the cell to the extracellular space (5).

Mice express two genes encoding Mdr1, *mdr1a* (also called *mdr3*) and *mdr1b* (also called *mdr1*) (12). In humans, a single MDR1 product displays both functions of murine Mdr1a and Mdr1b (13). Therefore, the physiological function of MDR1 in human has been deduced from the phenotype of mice in *mdr1a* and *mdr1b* gene knockout studies. Based on the analysis of mice with a genetic disruption of *mdr1a*, *mdr1b* or both *mdr1a* and *mdr1b*, it has been suggested that these genes are not essential for organ development but play important roles for drug transport (14–16).

In cancer, MDR1 activity appears to be the major reason for failure of chemotherapy; therefore, research has focused on the mechanism of drug resistance. However, recently, MDR1 has been suggested to directly associate with malignant proliferation of cells. One line of data showed involvement of Mdr1 in intestinal tumourigenesis through association with the tumour suppressor APC pathway (17). Therefore, MDR1 may regulate cell proliferation in tumours, although lack of MDR1 did not affect normal cell development in gene knockout studies (14, 15). In this study, we report suppression of tumour cell proliferation by down-regulation of Mdr1 in cancer cell lines.

MATERIALS AND METHODS

Cells—Mouse rectum carcinoma cell line Colon 26 cells were cultured in RPMI 1640 medium supplemented with 10% heat-inactivated fetal bovine serum (FBS; Sigma, St Louis, MO, USA). Mouse skin melanoma cell line B16 cells were cultured in DMEM medium supplemented with 10% heat-inactivated FBS. Fibroblast-like cell line OP9 derived from mouse calvaria was cultured in αMEM medium supplemented with 20% heat inactivated FBS. Mouse embryonic fibroblasts (MEFs) were prepared from

*To whom correspondence should be addressed. Tel: +81 6 6879 8316, Fax: +81 6 6879 8314.
E-mail: ntakaku@biken.osaka-u.ac.jp